Title
Limitation of one-dimensional models of sedimentation and thickening

Author
Li, Ben

Publication Date
2012

Peer reviewed|Thesis/dissertation

UNIVERSITY OF CALIFORNIA
LOS ANGELES

Limitation of one-dimensional models of sedimentation and thickening

A thesis submitted in partial satisfaction of the requirements for the degree Master of Science in Civil Engineering

by

Ben Li

2012

ABSRACT OF THE THESIS

Limitation of one-dimensional models of sedimentation and thickening

by

Ben Li

Master of Science in Civil Engineering
University of California, Los Angeles, 2012
Professor Michael K. Stenstrom, Chair

The earliest one-dimension dynamic clarifier model is established on the basis of mass conservation law for an ideal clarifier composed of a finite number of layers, and is used to simulate both underloading and overloading conditions. The estimation results indicate the original model can provide a sound predication in an underloading situation, but fails in identifying the sludge blanket level and underflow solids concentration in an overloading situation. Two improved models: the gravity flux constraint model and the dispersion model have been used to simulate both underloading and overloading conditions in order to test their reliability. Even though both of them can show the rise of sludge blanket height under the condition of overloading, their simulation results do not converge. Another obvious flaw of these two models is their sensitivity to the number of model layers, which means the simulation outcome is a

function of the number of layers. This inappropriate phenomenon has been demonstrated by testing these two models in 10-layer, 30-layer and 50-layer situations， and the variation tendencies of their simulation outcomes are opposite. Method of characteristic (MOC) is a kind of numerical methods used to solve nonlinear hyperbolic partial differential equation. Given the fact that the original model is a nonlinear first-order hyperbolic partial differential equation, MOC is applicable to solve it. However, a brief analysis illustrates the mass conservation equation can only provide a positive characteristic line, and the negative line remains unknown. A possible method to figure out the negative one is set another equation based on the momentum or energy conservation.

The thesis of Ben Li is approved.

Eric M.V. Hoek

Keith D. Stolzenbach

Michael K. Stenstrom, Committee Chair

University of California, Los Angeles

2012

LIST OF TABLES

Table.1—Data for the simulated WWT plant ……..45

Table.2—The key variables for Gravity Flux Constraint Model and Dispersion Model in the underloading situation……..64

Table.3—The key variables for Gravity Flux Constraint Model and Dispersion Model in the overloading situation……65

LIST OF FIGURES

Figure 1—Gravity settling velocity of Takács…….48

Figure 2—Gravity settling flux……49

Figure 3—Total flux and bulk flux……..50

Figure 4—Solids concentration profile (the original model, underloading condition)…….53

Figure 5—A dynamic solids concentration profile as a function of time and height(the original model, underloading condition)…….53

Figure 6—Solids concentration profile (the original model, overloading loading condition)……54

Figure 7—A dynamic solids concentration profile as a function of time and height(the original model, overloading condition)……54

Figure 8—Solids concentration profile (gravity flux constraint model, underloading condition)……60

Figure 9—A dynamic solids concentration profile as a function of time and height(gravity flux constraint model, underloading condition)…….60

Figure 10—Solids concentration profile (dispersion model, underloading condition)……..61

Figure 11—A dynamic solids concentration profile as a function of time and height(dispersion model, underloading condition)…….61

Figure 12—Solids concentration profile (gravity flux constraint model, overloading condition)……..62

Figure 13—A dynamic solids concentration profile as a function of time and height (gravity flux constraint model, overloading condition)……...62

Figure 14—Solids concentration profile (dispersion model, overloading condition)……..63

Figure 15—A dynamic solids concentration profile as a function of time and height (dispersion model, overloading condition)……..63

Figure 16—Solids concentration profile (gravity flux constraint 10-lyaer model, underloading loading condition)……68

Figure 17—Solids concentration profile (gravity flux constraint 30-lyaer model, underloading loading condition)……68

Figure 18—Solids concentration profile (gravity flux constraint 50-lyaer model, underloading loading condition)……69

Figure 19—A dynamic solids concentration profile as a function of time and height (gravity flux constraint 10-layer model, underloading condition)……...69

Figure 20—A dynamic solids concentration profile as a function of time and height (gravity flux constraint 30-layer model, underloading condition)……..70

Figure 21—A dynamic solids concentration profile as a function of time and height (gravity flux constraint 50-layer model, underloading condition)……..70

Figure 22—Solids concentration profile (dispersion 10-layer model, underloading condition)…….71

Figure 23—Solids concentration profile (dispersion 30-layer model, underloading condition) ……...…….71

Figure 24—Solids concentration profile (dispersion 50-layer model, underloading condition)…….72

Figure 25—A dynamic solids concentration profile as a function of time and height (dispersion 10-layer model, underloading condition)……..72

Figure 26—A dynamic solids concentration profile as a function of time and height (dispersion 30-layer model, underloading condition)……..73

Figure 27—A dynamic solids concentration profile as a function of time and height (dispersion 50-layer model, underloading condition)……..73

Figure 28—Solids concentration profile (gravity flux constraint 10-lyaer model, overloading loading condition)……..74

Figure 29—Solids concentration profile (gravity flux constraint 30-lyaer model, overloading loading condition)…….74

Figure 30—Solids concentration profile (gravity flux constraint 50-lyaer model, overloading loading condition)…….75

Figure 31—A dynamic solids concentration profile as a function of time and height (gravity flux constraint 10-layer model, overloading condition).

…….75

Figure 32—A dynamic solids concentration profile as a function of time and height (gravity flux constraint 30-layer model, overloading condition).

……..76

Figure 33—A dynamic solids concentration profile as a function of time and height(gravity flux constraint 50-layer model, overloading condition)..

……..76

Figure 34—Solids concentration profile (dispersion 10-lyaer model, overloading loading condition)……..…77

Figure 35—Solids concentration profile (dispersion 30-lyaer model, overloading loading condition)……..77

Figure 36—Solids concentration profile (dispersion 50-lyaer model, overloading loading condition)……..78

Figure 37—A dynamic solids concentration profile as a function of time and height(dispersion 10-layer model, overloading condition)…….78

Figure 38—A dynamic solids concentration profile as a function of time and height(dispersion 30-layer model, overloading condition)…….79

Figure 39—A dynamic solids concentration profile as a function of time and height(dispersion 50-layer model, overloading condition)…….79

Figure 40—The sketch profile of the characteristic line……...83

ACKNOWLEDGEMENTS

I want to express my deepest appreciation to my advisor Dr. Michael K. Stenstrom, not only for his guidance and assistance in developing this thesis, but also for his patience and encouragement. His encyclopedic knowledge stimulates my motivation to conduct the study and finish the thesis.

I also want to thank the rest members of my thesis committee: Professor. Keith D. Stolzenbach and Professor. Eric M.V. Hoek. The comments made by the committee greatly improve my understanding of this study, and I really appreciate their kind help.

Finally, without my parents Xiubao Li and Zhenhui Wang, my girlfriend Linling Shen’s irreplaceable love, I can never finish this thesis. I wish to express my gratitude to them.

CONTENT

1. INTRODUCTION 1

2. LITERATURE REVIEW 6

2.1. Background of the Secondary Clarifier 6

2.2. Brief Review of Thickening Theory 7

2.2.1. Development of Thickening Theory 7

2.2.2. Verification of Kynch Theory 14

2.3. Investigation of the Continuous Settling Process 18

2.4. Mathematic Modeling of the Sedimentation Process 21

3. RESULTS AND DISCUSSION 41

3.1. Original Dynamic Settling Model 41

3.1.1. Rebuilding the Original Dynamic Settling Model 41

3.1.2. Simulation of the Underloading and Overloading Conditions 44

3.2. Modification of the Original Dynamic Model 55

3.2.1. Gravity Flux Constraint Model and Dispersion Model 55

3.2.2. Simulation of the Underloading and Overloading Conditions 57

3.3. Flaws of Gravity Flux Constraint Model and Dispersion Model 64

3.4. Summary of Existing One-Dimensional Clarifier Models 66

3.5. Method of Characteristics 80

3.6. Possibility and Difficulty of Using Method of Characteristics 81

4. CONCLUSION 85

REFERENCE LIST 88

1. INTRODUCTION

A major advance in water quality protection in the United States occurred with the passage of the Clean Water Act Amendments in 1972, which required all dischargers to met treatment goals of 85% five-day biochemical oxygen demand (BOD_5) and total suspended solids (TSS). Prior to 1972, many US cities only had primary treatment. In most cases, upgrading the primary treatment requires a biological secondary treatment process, which is highly dependent on the ability of microorganisms to convert dissolved organic material into suspended material and to bioflocculate fine colloidal material into larger particles or flocs. Biological secondary treatment processes are now widely used in wastewater treatment plants to remove organic matter and sometimes to reduce nutrients such as nitrogen and phosphorus [1]. The produced biomass removes nutrients by oxidation or incorporation. In all cases, efficient operation requires the biomass to be removed from the wastewater by sedimentation, filtration or other solids-liquid separation process.

For sedimentation to be successful, the biomass must be composed of large particles or flocs which have sufficient settling velocity to be removed in a clarifier of manageable size. To achieve this goal it is necessary to grow the biomass to select floc-forming organisms as well as understanding clarification process to create well-designed clarifiers. Reactor designs are now optimized to select floc-forming organisms as

opposed to filamentous or foam-producing organism.

The biomass leaving the reactor is a mixture of biosolids and water, commonly referred to as a slurry or sludge. The separation of slurries can be achieved by several types of treatment processes, but secondary clarifiers are most commonly used. Secondary clarifiers, also known as sedimentation basins or solids-liquid separators, use gravity to separate the biosolids from the fluid, and have two similar but distinct functions: clarification and thickening.

Clarification is the removal of finely dispersed solids from the liquid to produce a low turbidity, low TSS effluent. Thickening is the process of increasing the biosolids concentration in slurry in order for it to be recycled or disposed in less volume. Both depend on the small differences in specific gravity of the biosolids and water. In clarifiers, the clarification process occurs in the upper zone while thickening occurs near the bottom. The result is an effluent from the top, low in suspended solids, and a second stream of settled, concentrated solids from the bottom, suitable for recycling or disposal.

As one of the most important units in wastewater treatment process, the performance of a secondary clarifier often determines the capacity of a wastewater treatment plant (WWT). If the clarifier does not remove solids from the effluent, or fails to produce a recycle stream, process failure invariability occurs with effluent permit violations and loss of biomass from the reactor. Therefore, two commonly used design parameters: overflow rate and solids flux, have been developed to evaluate and design

clarifiers. Using these two parameters, engineers have created design and operation strategies for treatment processes by accounting for secondary clarifier limitations in order to provide high-quality, stable operation.

Nevertheless, given the fact that the wastewater characteristics vary, such as flow rate and contaminant concentrations, traditional design procedures for secondary clarifier tend to be a more empirical and conservative by introducing averaged parameters with safety factors. Therefore secondary clarifier performance can suffer unanticipated fluctuations, which may cause secondary treatment control problems and increase the risks of failure. Stringent standards for effluent quality and urgent need for optimization of WWT performance have made such variations in effluent quality undesirable, and have encouraged the use of dynamic controls for wastewater treatment process. For the purpose of developing such an automatic control system to provide for uniform effluent water quality, a great amount of work has been performed to create accurate mathematic descriptions of wastewater treatment process, and the dynamic one-dimension model for predicting the time dependant responses to transient process inputs of secondary clarifiers is a good example.

One-dimension clarifier models (1-D model), based on solids-flux theory, describe sludge transport by a mass conservation first-order partial differential equation. Several other extension factors: continuous settling, constraints of sedimentation flux from layer to layer, compressive effects and dispersion terms have been introduced to the initial equation in order to provide better agreement between model results and lab or full scale

observations. Although many 1-D models are available and some of them, especially Takács' 10-layer model [2], have been widely utilized in engineering practice, the predication of the sludge settling characteristics and concentration profiles in and out of the clarifier are still far from satisfactory for practical purposes, due to obvious shortcomings and dilemmas.

Firstly, the presently available 1-D models are highly dependent upon empirical equations to express clarification, thickening and compaction process and these equations or functions are an error source and can profoundly affect simulation results. A second challenge is the difficulty of making full-scale measurements on working clarifiers which has created a lack of data sets for model calibration and verification. This helps explain why previous work tends to use empirical equations, especially for the calculation of hindered settling velocity and compression. As a consequence, further research is still needed to improve the performance of the 1-D model.

The goal of this thesis is to extend the knowledge of clarifier performance in order to improve 1-D models and especially to show their utility in predicting clarifier performance and failure conditions. An extensive literature review is provided, covering the classical, steady state research that has lead to the well-applied solids-flux theory of clarifier operation. From this foundation, 1-D clarifier models are reviewed and different available models are tested under various flux loading conditions. These models are then used to simulate practical situations, such as

time-to-failure after overloading. Finally, suggestions for additional research are provided.

2. LITERATURE REVIEW

2.1. Background of the Secondary Clarifier

As one of the most important units in a wastewater treatment plant, the secondary clarifier is often a “bottle neck,” limiting the capacity of the wastewater treatment process. Clarifier sizing must be combined with the aeration basin sizing to guarantee the minimum performance of secondary wastewater treatment pants, as well as maximizing its efficiency for contaminants removal. The significance of the final clarifier can be attributed to its three major functions: clarification, thickening, and storage.

Clarification, occurring in the upper part of the clarifier, above the feed point (hence it is called the clarification zone) separates the suspended solids from wastewater flow by specific gravity differences to produce an effluent low in TSS concentration. A concentrated underflow must be obtained during the thickening process below the feed point, and the settled slurries must be transported to the bottom of the clarifier where they are removed and recycled to the aeration basin to maintain the mixed liquor suspended solids concentration. Storage refers to the function of temporary slurry storage during the changes in wastewater flow rate, such as the diurnal variations common in domestic treatment plants or upsets or shock loads. Storage prevents process failure by retaining the biosolids during short term flow variations.

In spite of improved knowledge and recent modeling advances, the final

clarifier still remains a sensitive and complicated unit in an activated sludge treatment plant, and sometimes will suffer an unexpected failure deteriorating the overall efficiency of the treatment plant.

Given these problems, a proper design and operating strategy for secondary clarifiers is an essential backbone of a wastewater treatment plant. A validated, user-friendly model for evaluating and predicting the behavior of the final clarifier will contribute to understanding the final clarifier's responses to variable operating conditions such as loading rate, overflow rate, withdraw flow rate and upsets. Numerous studies aimed to develop better designing and operating strategies, some with mathematical models, have been carried out, with the goal of improving engineering understanding of secondary clarifiers, hopefully achieving more reliable and efficient activated sludge treatment plants.

2.2. Brief Review of Thickening Theory

2.2.1. Development of Thickening Theory

Most early investigations for developing design and operating equations to predict the possible behavior of the secondary clarifier were based on the understanding and utilization of classic batch thickening tests results, which were believed to supply all necessary information for clarifier design and operation. In these classical experiments, a suspension of particles of known concentration was added into a graduated cylinder and thoroughly mixed by stirring. After mixing, the particles were allowed to

settle, and the height of the interface between the clear supernatant and particles was recorded over time. Coe and Clevenger (1916) conducted one of the pioneering works showing how a batch settling test can be used in the secondary clarifier design and operation. This classical methodology exerted a profound impact on clarifier design over the next half century [3].

With qualitative expressions, Coe and Clevenger firstly distinguished the four zones generated during batch settling tests in cylinder column [4]. The first zone named clear water zone was a clear supernatant in low suspended solids concentration. Underlying the first zone, the secondary zone had a similar concentration as the initial feed MLSS. The third zone was a transition zone between the constant solids concentration zone (the second zone) and the fourth zone known as compression zone due to the compression effect caused by a relative higher solids concentration compared with the other three zones. Since similar classification of zones can also be found in a real continuous thickener[5], the study of the batch settling test can be used to estimate the real situation of the secondary clarifier[4]. Identifying the constant solids concentration zone and the transition zone as two free settling zones different from the compression zone, Coe and Clevenger divided the continuous settling process into two distinct stages: free settling governing the clarifier area requirement, and compressive settling determining the requirement of the depth of the thickening zone [3].

Another important conception discussed in Coe and Clevenger’s classical

paper was the solids handling capacity, now known as solids flux-density. Their observations demonstrated the ability of one layer with certain solids concentration to convey solids flux to the next layer showed a maximum value [4] . The minimum value of all layers was the upper limit of feed flux the clarifier can handle, also known as the maximum feed flux that can be transmitted to the bottom of the clarifier. To determine the solids handling capacity based batch settling tests, Coe and Clevenger provided an empirical relationship. Tracy [3]modified it by expressing it in terms of concentration units as equation 1.

$$C = \frac{V_i}{\frac{1}{c_i} * \frac{1}{c_u}} \quad (1)$$

Where C = solids handling capacity or the maximum flux which can be transmitted; c_i = solids concentration of the layer under consideration; c_u= desired underflow solids concentration; V_i = gravity settling velocity of a solids suspension has a concentration. As mentioned above, the layer having the minimum flux handling capacity determined the requirement of thickener area. Since equation 1 expressed this special layer as well as its solids concentration, it became a basic mathematic approach to calculate the area requirement for the secondary clarifier. Once the gravity settling velocity was determined, the area can be calculated.

Coe and Clevenger were not so specific in the subject of selection the depth of the thickener as they were in determining the requirement of the clarifier size [3]. Using a simple hypothesis that the loss of water or the

sludge compaction level in the compression zone was a function of time, Coe and Clevenger suggested that a more desired withdrawal concentration can be obtained with a sufficient depth by providing a longer compacting time. Even though Coe and Clevenger emphasized the great practical value of conducting batch settling tests in predicting the probable behavior of the secondary clarifier, they also stated that conducting batch tests was not enough; one has to perform continuous thickening tests for a satisfactory evaluation [3].

Coe and Clevenger's empirical design procedure was widely accepted and further extended due to its simplicity and practicality, and was the only available quantitative design method during the first half of the 20^{th} century. This design strategy was prevalent and dominant until a more theoretical description of the batch settling process was presented by Kynch in 1951 [6]. To entirely describe the settling process without an intricate mathematic expression and the necessity of knowing actual forces on the particles in detail, Kynch made two types of assumptions as followings:

1. The particle concentration is uniform across any horizontal layer.

2. The initial concentration increases towards the bottom of the "dispersion."

3. The velocity *v* tends to zero as ρ (density) approaches to ρ_m (maximum density).

4. The velocity of fall depends only on the local particle density.

5. Wall effects can be ignored.

6. The particles are of the same size and shape.

In his celebrated paper, Kynch gave an analysis of each assumption, except the fundamental assumption 4, and recognized the fact that it was impossible to verify the validity of this hypothesis until the details of the forces on the particles can be specified. The settling process was represented by the continuity equation of the solids phase:

$$\frac{\partial \rho}{\partial t} + V_{(\rho)} \cdot \frac{\partial \rho}{\partial x} = 0 \qquad (2)$$

Where ρ = the local concentration of particles (the number of particles per unit volume of the dispersion); V = the velocity of fall, a function only of the local concentration ρ of particles; X = the height of any level above the bottom of the column of dispersed particles; equation 2 can be further discussed by the mathematical technique of using the characteristics of a partial differential equation with proper initial and boundary conditions[7]. Therefore, the discontinuous settling behavior can be analyzed based from equation 2 without knowing the precise mechanism of different settling methods [7].

Kynch also described the formation and propagation of the particle concentration discontinuity, occurring in the zone settling, by introducing the following expression:

$$U = \frac{S_1 - S_2}{\rho_1 - \rho_2} \tag{3}$$

Where U = the upwards velocity of the discontinuity; S = Settling Flux; ρ = the local concentration of particles (the number of particles per unit volume of the dispersion). Kynch's theory is a great breakthrough, since it contributes greatly to the understanding of the batch settling process and promotes the development of clarifier thereafter.

However, what Kynch did not analyze was the relationship between batch settling tests and continuous thickeners [8]. Therefore, for the purpose of integrating Kynch's theory and real continuous thickener design, Talamge and Fitch[8] developed a designing procedure after demonstrating the validity of Kynch's analysis.

Using various settling materials, Talamge and Fitch performed a series of batch settling tests with different initial concentrations. The experimental data sets were analyzed by the Coe and Clevenger procedure and Kynch procedure respectively. The results showed that the Kynch method was always as good as the Coe and Clevenger method, and in many cases, the Kynch theory was better. The field observations also showed a good correlation with Kynch theory [8]. Afterwards, Talamge and Fitch [8] developed a new design strategy based upon an extension of Kynch theory, suggesting that the slope of the tangent to the interface subsidence curve of a batch settling test is equal to the settling velocity of the layer which has the same solid concentration. They also followed Coe and Clevenger's suggestion that only free settling zones govern the unit area requirement.

The technique can be expressed as the following equation:

$$\text{Unit Area} = \frac{t_u}{C_0 \cdot H_0} \tag{4}$$

Where *Unit Area* = the area required to allow one ton of solids to settle through the layer concentration in one day; C_0 = the initial concentration of a column of pulp in a batch settling test; H_0 = the initial height of a column of pulp in a batch settling test; t_u = the time for the total quantity of solids to subside past through the layer, propagated up from the bottom of the column. Equation 4 indicated that the Talamge-Fitch design procedure was dependent upon precisely determining the compression point, t_u. However, Talamge and Fitch did not give any suggestions to evaluate t_u. Lots of approaches have been proposed by other scholars, but most of them are empirical [9-11] .

Beyond the lack of theoretical methods to determine the compression point, t_u, an obvious drawback of Talamge-Fitch procedure is a tacit assumption that the solids handling capacity of the thickener is controlled by the concentration which exists at the liquid-solid interface at the moment when all solids pass through into the compression zone [3]. The correctness of this fundamental but tacit assumption still remains unclear.

Subsequently, environmental engineers observed an unexpected problem that this design method was conservative, underestimating the solids handling capacity of a real thickener, and always caused some unfavorable results, such as oversizing.[1, 12] Even Fitch himself admitted that the

solids handling capacity estimated by this method was drastically less than the real one. Aldeton demonstrated this result showing that the experimentally observed flux can be 1.5 times larger than the estimated flux [1, 13]. One possible explanation of this underestimation is that during the compression, the settling velocity is no longer only a function of the concentration, contradictory to the original Kynch hypothesis [3]. However, in spite of the tacit assumption and conservative tendency, Talamge-Fitch Method was still advocated by many practitioners, because of its improved veracity, especially compared with Coe and Clevenger multiple batch settling tests method [14-17].

2.2.2. Verification of Kynch Theory

In Talamge and Fitch's paper, the Kynch theory, particularly the assumption that the free settling velocity is a function only related to the solids concentration has demonstrated its value as a powerful and feasible approach transforming the intricate batch settling process to a simple mathematic expression. However, in consideration of the possibility of creating conservative design and other unfavorable problems, additional research was motivated to demonstrate the validity of the Kynch theory. Most researchers focused on the ability of the free settling velocity obtained in laboratory scale batch settling conditions can accurately represent the observed velocity in the full-scale continuous thickeners. Due to the limitation of experiment conditions, such as the small settling vessel, the continuous stirring for complete mixing, and the limited number of slurries, the experimental conditions, such as the diameter of

the cylinder and the initial height of tested slurries, can be greatly magnified.

When the diameter of the batch test container becomes fairly small with respect to the diameter of the particle, the particles or the flocs within the slurries will tend to form “bridges” or “arches” between the walls to that creates a mechanical support force to deter the settling or reduce the settling velocity. Once the collapse of the “bridges” or “arches” occurs because of the overweight slurries, an accelerated settling of the interface of the slurries will be observed. Another impact from the wall effect is the movement of liquid along the cylinder wall rather than through the more circuitous path of the slurry. In this instance, the water loss is more rapid than normal, and the apparent subsidence velocity is noted to be higher than would occur in a larger container [3]. The impact of wall effect has been confirmed by Vesilind (18) with compressive data showing that a small diameter cylinder can produce a higher settling velocity for dilute suspensions, while decreasing the velocity with concentrated suspensions. Based on these notable experiment results, Dick [18] stated that increasing the diameter of the cylinder can decrease the settling velocity in batch settling tests, and the diameter effect tended to be more apparent with concentrated suspensions than the dilute ones. Based on the preceding discussion, the cylinder with a larger diameter is preferable, but the utilization of larger cylinders requires a greater volume of fresh slurries for batch settling tests, and presents a new problem of how to maintain a uniform initial settling concentration through the cylinder without introducing turbulence, which may alter the subsidence characters of the

slurries[3]. To avoid altering the subsidence characteristics and to avoid the difficulty of managing large volumes of slurries, cylinders with small diameter are more wildly applied in real batch settling tests, ignoring any potential wall effects.

To offset the impact of wall effects, a slow speed mixer has been introduced. It has been shown that a slow speed stirrer will not impose the settling velocity of dilute slurries [3]. Dick further demonstrated that mixing process was indispensible to counteract the influence of the wall effect, when the slurries concentration exceeded 6000 to 7000 mg/l[18].

The possible impacts upon the solids settling characteristics also have been estimated. Kammermayer [19] found that the slow stirring process can produce more compact final slurries, supported by Eckenfelder and Melbinger [11]. Nevertheless, many researchers record free settling velocity using a stirrer in the batch settling tests. As a result, extending the mixture to the entire depth of the batch settling column has been strongly recommended by a lot of researchers, while the stirring in most cases show more profound effect in the zone with relative high concentration[20, 21]. Another result of stirring is that it provides a more uniform initial settling concentration through the cylinder column and prevents a subsidence lag time from occurring.

The Kynch theory has also been questioned a lot, since it did not consider the relationship between the settling velocity and the initial height of the slurries suspension. Several experiments have been designed to evaluate the effect of height by conducting the settling tests at different initial

settling heights. The experiment results showed that the initial settling height can greatly alter the settling character of the slurries, and a higher initial height brings better settling characters [19, 21]. Dick made an assessment of the initial height effects and concluded that increasing the initial height six feet greatly improved the subsidence velocity, which contradicted to Kynch theory totally [18]. However, after changing the settling materials from activated sludge to sand, the experiment results tended to support Kynch theory that the settling velocity is independent of the slurry height [18]. The discrepancies of experiment results can be attributed to the fact that activated slurries deviate greatly from Kynch's fundamental assumption that the ideal settling particles having uniform shape and size, while sand meets this assumption much better [3].

Further studies have been conducted to ascertain the validity of Kynch's analysis by using more ideal particles. By doing a series of batch settling tests, Shannon and Tory [22] demonstrated that experimental batch settling behavior of rigid spheres in water was found in qualitative and near quantitative agreement with settling behavior predicted from a solids flux plot assuming that the solids settling velocity is a function of solids concentration only. The small observed deviations were believed to be caused by the slightly non-uniform initial concentration and the particle segregation effect in dilute concentrations. Solids having a Gaussian distribution show that no noticeable segregation at reduced concentrations of 0.15 (C_i/ρ_s) or higher, therefore the assumption of uniform shape and size particles no longer constrains the Kynch theory [22].

One of the major criticisms to Kynch theory was that it was difficult to predict the settling behavior at a high slurries concentrations, especially the subsidence occurring in the compression zone[3]. Conducting batch settling experiments with calcium carbonate slurries having initial concentration at compression concentrations (> 145 g/L) indicated the settling velocity was still largely determined by the local solids concentration, and the solids profiles were fairly similar to the ones predicted by Kynch theory for rigid sphere [23]. The mechanical stress was believed to be the major reason for the gradual increasing of concentration and the curved concentration profiles near the bottom area [23].

2.3. Investigation of the Continuous Settling Process

Most previously discussed cases were focused on the study of batch settling process, and scholars believed that the classical batch settling tests can provide almost all information to describe the continuous settling process. With the attempt to evaluate how the operating or controlling factors were related to the subsidence behavior, certain experiments were carried out to observe the behavior in the compression and settling zones[24] . To control the detention time and the depth of the compression zone, Coming [24] in his experimental investigation, chose feed flow rate and the underflow rate as variables, demonstrating that the underflow concentration was negatively correlated with the underflow rate. He also

showed that increasing the detention time or the depth of the compression zone can increase the underflow solids concentration. Coming also compared the effects of two different rake mechanisms: a standard rake and a picket rake (with vertical bars extending above the rake), and found that no discontinuity in the concentration-height curve was observed, as well as a more uniformly increasingly concentration using a picket rake. Another interesting observed experiment phenomenon was a zone of constant solids concentration was produced with successive increases in feed flow rate with constant underflow rate. Coming emphasized the importance of this zone controlling the limiting capacity of the thickener, since it determined the rate at which the solids reached the compression zone[24].

Yoshioka [25] supported the assumption that batch tests can provide sufficient information to describe continuous thickening. Yoshioka's most important contribution was to provide graphical analysis method of batch flux data, and showed how it can be used to predict the underflow concentration. His procedure is the most accepted method today. His statement that the subsidence occurring in the compression zone was not due to the compression effect, but just a function of the solids concentration in that zone, was in accordance with Kynch theory. By expressing the settling rate as a function only related to the local solids concentration, the underflow concentration can be predicted based on the limiting solids handling capacity and underflow velocity, and it was the first analytical approach to predict the underflow concentration [3]. The discrepancies between Yoshioka and Coming are the perspective of the

function of detention time and compression zone depth upon the underflow concentration. Yoshioka concluded that neither the thickness of compression zone nor the detention time affected the underflow concentration[25].

Hassett [26] developed an analyzable method to evaluate the settling capacity of a specific thickener. By conducting numerous continuous thickening tests with various settling slurries, Hassett found that both the requirement of size and the underflow concentration can be briefly estimated from the minimum point from the total flux curve, such as Figure 3. He derived a quantitative expression to explain the independence of the concentration discontinuity and the mechanical agitation, and confirmed that the slurry depth was unrelated to the settling behavior. He showed that a rising of slurry blanket did not increase the underflow concentration when feed flow was increased which was in conformity with Yoshioka's conclusion based on the analysis of batch settling tests[26].

Yoshioka's batch flux diagram was extended to a double concave flux diagram by Shannon and Tory. The double concave flux diagram demonstrated that two stable constant solids concentration zone can exist in a continuous thickener [27, 28] . Opposite to Coming's conclusion, Shannon and Tory found that the detention time had no relationship with the settling behavior, and the underflow rate was the determining factor of underflow concentration [27].

The existence of two constant solids concentration zones under a critical

or overloaded condition has been confirmed by Dick and Javaheri [29]. The observed concentration profile was approximate to the theoretical one with two constant solid concentration zones presented in Shannon and Tory's paper[23]. With the goal of investigating the non-ideal slurries concentration profile, Javaheri introduced a mixture containing calcium carbonate, lime softening sludge and activated sludge as a compressive and non-ideal slurries sample. Though there were small quantitative deviations between the observed concentration profile and the predicted one, basic agreement was obtained, confirming the soundness of the predication strategy [30].

2.4. Mathematic Modeling of the Sedimentation Process

Although a number of continuous settling studies have been conducted, almost no research was performed to describe the settling process using continuous differential equations. Several empirical models, such as Edde and Eckenfelder model and the model recommended by the Environmental Protection Agency, were developed, and they all contained specific empirical parameters, resulting in unexpected deviations between the simulation results and real data sets [31].

The first attempt to develop a dynamic model for continuous thickening was presented by Bryant [32]. Bryant's idea was divide the clarifier into several layers along vertical direction, and the total flux in and out of each layer was separated into two parts: the bulk flux, caused by the underflow, and gravity flux, caused by the gravity settling. By the use Kynch theory,

Bryant generated the following partial differential equation upon the basis of mass conservation law:

$$\frac{\partial C}{\partial t} = -\left(u + \frac{\partial G_s}{\partial \mathrm{C}} \right) \cdot \frac{\partial C}{\partial Z} \qquad (5)$$

Where C = the solids concentration in each layer; t =time; u=the underflow rate in the thickening zone; G_s = the gravity flux of each layer and Z =the vertical distance in the thickener.

Simulating underloading conditions confirmed the existence of constant solids concentration zone below the feed layer which was in accordance with Kynch theory. Since the operation flux was transmitted to the bottom of the thickener and went back to the aeration tank, steady state conditions were maintained in the thickening zone [32]. Neither the clarification zone nor an overloading condition was investigated, although both are essential to estimate the effluent solid concentration and prevent thickener failure.

Instead of analyzing the solids concentration layer by layer as Bryant[32], Tracy developed an inventory model[3]. In implementing the inventory model for the continuous thickening process, the vertical section of the thickener was considered as four different zones with variable volumes. The area above the feed point was named the clarification zone, due to its relatively low suspended solids concentration.. The second zone, called the dilution zone, extended from the inlet downward to the sludge blanket surface. Beneath the dilution zone was the portion of the thick blanket,

called thickening zone, usually with a constant and uniform concentration. Both the existence of the dilution zone and thickening zone were dependent upon the loading conditions. The bottom was called the compression zone and contained the rapidly increasing solids concentration. Mass conservation equations were built in order to describe the change of height and solids concentration in each zone. For example, equation 6 was used to predict the level of sludge blanket in overloading condition.

$$\Delta Z = \frac{(G_{in} - G_{out})}{C} \cdot Delt \qquad (6)$$

Where G_{in} = settling flux into the thickening zone; G_{out} = settling flux out the thickening zone; C = the solids concentration in thickening zone; *Delt* = simulation control increment, normally 0.01 h; ΔZ = the level variation of sludge blanket height. The essential foundation of Tracy's model was the identification of four different zones with different properties and solids concentrations, and the zone definitions were based upon Hassett's observations[12].The zone heights and their concentration were calculated from mass balances, as opposed to using discrete layers, as Bryant did[32]. Tracy's model provided an inventory of the solids in the sedimentation tank, and could be used to predict clarifier overloading.

Stenstrom modified Bryant's model, because he observed that Bryant's continuity model could not predict clarifier overloading [33]. In order to model the overloading condition, especially for estimating the sludge blanket level, Stenstrom gave the following assumptions:

1. The dispersion is zero (plug flow).

2. The mass flux flows into a differential volume can never exceed the flux which the volume is capable of passing nor it can exceed the next higher differential volume is capable of transmitting.

3. The settling velocity is a function only of the solids concentration, except when assumption 2 is violated.

4. The bottom of the clarifier represents as physical boundary to sedimentation; therefore the settling flux at the bottom of the clarifier is zero.

5. The solids concentration is completely uniform in any horizontal plane.

6. There is no biological reaction in the separator.

The assumption 2 is the most significant one, because it exerts an extra restriction to the gravity settling flux, which the original continuity model does not contain. So, Stenstrom wrote the following equation based on the mass conservation law around each layer.

$$\frac{\partial C}{\partial t} = v_u \frac{\left(C_{i-1} - C_i\right)}{dz} + \frac{\left(\min\left(G_{i-1}, G_i\right) - \min\left(G_i, G_{i-1}\right)\right)}{dz} \quad (7)$$

Where C = solids concentration; v_u = bulk downward velocity; G_i = the gravity settling flux in layer i; dz = the thickness of each layer. Stenstrom demonstrated that the modified model was capable of simulating the

overloading condition much better than the original continuity model[33]. With the thought that a thickening failure will occur when the sludge blanket level exceeds the feed point, Stenstrom did not simulate the settling behavior in the clarification zone.

Vitasovic noticed that the dynamic model developed by Bryant and modified by Stenstrom was effective in predicting the underflow concentration, but believed that it failed in estimating the sludge blanket height under different feed flux conditions. The strategy for thickening zone simulation was similar to Stenstrom's model, except an introduction of one special threshold C_t, the concentration of the certain layer that the solids flux of this given layer can affect the settling flux in the next upper layer. The top layer of the sludge blanket was defined as the closest layer to the top of the clarifier with the concentration equal or greater than the C_t [34]. To model the clarification zone, Vitasovic assumed that the precondition for a successful settling required the gravity settling velocity to be larger than the upward flowrate or overflow rate, V_b, [34]. His model contained five zones or layers with potentially different solids concentrations: the top layer, the layer between the top and feed layer, the feed layer, the layer between the feed and the bottom layer and the bottom layer. Each layer was described by its each unique different equation. In his dissertation, Vitasovic presented the following suggestions to improve the model:

1. Modify the assumption that the radical concentration profile is uniform through the layer thus allowing a concentration gradient in

two dimensions rather than one.

2. Include the turbulence effects on the conveyance of solids between each layer.

3. Structure the solids with respect to the settleability.

4. Use a more realistic velocity profile.

His suggestions essentially are a proposal for a two dimension model with dispersion.

To evaluate the peak loading effects from the storm and snow-melt waters to the operation of the secondary clarifier, Laikari developed a dynamic model to the sludge blanket height deviations in various loading conditions[35]. The method to determine the level of the sludge blanket he used the method originally proposed by Tracy and Keinath. He improved the model by accounting for the conical shape of the clarifier, and by adding a turbulence effect by introducing a dispersion coefficient *D*. His use was unconventional in that he multiplied D times the first spatial derive of C. The strategy of handling the limiting flux was to transfer flux exceeding the limiting flux in a layer to the layer just above it. Instead of following Kynch theory to handle the gravity settling velocity (solids concentration only a function of concentration), the gravity settling velocity was determined by various batch settling tests and calibrations in Laikari's model [35] . According to obtained data sets from this model, a brief conclusion was that the influent solids flux, available solids storage

capacity and sludge settling velocity in the clarifier were the three major factors determining the efficiency and capacity of the clarifier [35]. Laikari also looked forward to combining the clarifier model with a possible aeration model.

One of the most well-known and widely used one-dimensional multi-layer dynamic models is Takács 10-layer model. Based on the solids flux theory and the mass conservation law around each layer, the equation was deviated as a first-order particle differential equation with the Stenstrom flux constrain for solids flux controlling in two adjacent layers. For the purpose of simulating the settling behavior in the clarification zone, Takács developed equation 8 to describe the settling velocity for both types of discrete and hindered sedimentation.

$$V_{sj} = V_0 \cdot e^{r_h \cdot X^*_j} - V_0 \cdot e^{r_p \cdot X^*_j} \qquad (8)$$

Where the V_{sj} = settling velocity of solids particles in layer j; V_0 = the maximum settling velocity; r_h = the settling parameter characteristic of the hindered zone; r_o = the settling parameter characteristic of the low concentration zone; X_j = suspended solids concentration in layer j; X_{min} = the minimum attainable suspended solids concentration; $X^*_j = X_j - X_{min}$ [2].Compared with Vesilind velocity equation[36], Takács velocity equation was able to work in both discrete and hindered concentration zones as shown in Figure 1. The steady state and dynamic simulation results have been verified using Pflanz's full-scale data and Thompson's pilot plant data. These verifications illustrated that the 10-layer clarifier

model can predict the concentration profile along the height of the clarifier, the effluent solids concentration, and the underflow concentration very well under both steady state and dynamic conditions. But, Takács also admitted that the modeling results were not so perfect since the mass of solids entering the clarifier was larger than the solids leaving the clarifier in an underloading situation[2].

Hamilton drew a conclusion on the previous dynamic clarifier models that the these models were based on the discretization of the first-order partial differential equation derived from the mass conservation law, and the drawback of the these models was that they failed in predicting the continuous variation of solids concentration with depth [37]. To remove this shortcoming, a second-order parabolic partial differential equation including a Fickian dispersion term was introduced, as show in equation 9, and the gravity settling velocity equation was Vesilind equation as equation 10.

$$\frac{\partial C}{\partial t} = -\frac{\partial G_s}{\partial Z} + U \cdot \frac{\partial C}{\partial Z} + D \cdot \frac{\partial^2 C}{\partial^2 C} \tag{9}$$

$$G_s = V_0 \cdot C \cdot e^{-b \cdot c} \tag{10}$$

Where V_0 and b = coefficients dependent on the settling characteristics of the sludge; C = the total particulate concentration; G_s = the gravity settling flux; D = a dispersion coefficient; ∂Z = the height of each layer [37]. The difference between Laikari and Hamilton dispersion equation is that Laikari's equation is a first-order partial differential equation, while

Hamilton's formulation corresponds to accepted dispersion model theory.

The predicted concentration profile supported Hamilton's assertion that the introduction of a dispersion term *D* enabled the prediction of the continuous variation of solids concentration in thickening zone. However, the shortcoming of the dispersion equation was that the simulation result was sensitive to the number of model layers, which was obviously inappropriate, a comment from Hamilton [37].

Not all of the dynamic models have been based on the flux theory. Hätel and Pöpel stated that under a steady state condition, the solids profile over the tank depth can not be derived from the solids flux theory, since the solids flux was independent of the depth Z [38]. A special gravity settling velocity equation was illustrated as equation 11:

$$V_s(ss) = V_{s.0} \cdot e^{-n_v \cdot ss} \qquad (11)$$

Where $V_{s.0}$ = the upper limit of gravity settling velocity, a function of the sludge volume index *(SVI)*; *SS* = the solids concentration; n_v = velocity parameter, a function of the sludge volume index *(SVI)*. In addition, to express the settling velocity for in domain of transition and compression, the velocity of hindered concentration zone was adjusted by a Ω correction function, which only dependent upon the position of compression h_c=*f(SVI)*, defined as the height as which the settling curve has the largest curvature [38]. Finally, they derived equation 12 to predict the concentration profile through the thickener:

$$\frac{dSS}{dZ} = \frac{-\frac{d\Omega}{dZ} \cdot V_{ss_z} \cdot SS_z}{\left[\frac{dV_s}{dSS} \cdot SS_z \cdot \Omega_z + V_{ss_z} \cdot \Omega_z + \frac{Q_{RS}}{A_{SC}}\right]} \quad (12)$$

Where Q_{RS} = the underflow rate; $A_{s\,c}$= the area of the thickener. With a further investigation of the possible application of this model, Hätel and Pöpel found that the integrated model including the clarifier model always gave a larger cell concentration predication in the aeration basin, but a smaller effluent solids concentration predication [38].

To forecast the possible response of a clarifier under dry and wet weather conditions, Otterpohl and Freund used the Hätel and Pöpel's Ω correction function's advantage in adjusting the gravity settling velocity at the domain of transition and compression, and Takács's 10-layer model's advantage in predicting the level of sludge blanket[39]. An important initial contribution made by Otterpohl and Freund was that they divided the solids in the secondary clarifier into two components: small solids and macro flocs, and modeled them respectively. The macro flocs settling velocity was determined by Härtel's velocity equation [38] and small solids had a constant velocity. The verification results indicated that the model roughly corresponded to the full-scale data. The deviation between the simulation result and the real data can be attributed to the change of slurries' settling characteristics in the combined water flow. An effective deviation reducing strategy was to set the volume of each layer at least one magnitude larger than the underflow volume in one time interval [39].

Another available dynamic model was presented by Dupont and

Henze[40]. In that model, the Vesilind equation was used to calculate the gravity settling velocity in the thickening zone. By dividing the clarifier into several horizontal layers and assuming there was no solids concentration gradient in horizontal direction, the limiting flux was calculated in each layer and compared with the feed flow from upper layer, similar to Laikari's strategy. Based on the influent characteristics of the clarifier, equation 13 was derived to describe the relationship between the effluent concentration and the MLSS in the aeration tank:

$$X_F = X_{\min} + X_{NO_3} \cdot \frac{X_{NO_3}}{K_{NO_3} + X_{NO_3}} + X_{hyd} \frac{X_{AT} \cdot SVI \cdot \frac{Q \cdot (1+r)}{A}}{K_{hyd} + X_{AT} \cdot SVI \frac{Q \cdot (1+r)}{A}} \qquad (13)$$

Where X_F = the effluent solids concentration; X_{min} = the constant solids concentration which always will be non-settleable; X_{AT} = MLSS in the aeration tank; Q_0/A = hydraulic load to the clarifier; SVI= sludge volume index; X_{hyd} = Monod constant for load. However, equation 13 was highly dependent upon the empirical observation and conceptual idea, and is difficult to use in practical cases.

A comprehensive comparison of the one-dimension dynamic models discussed above has been conducted by Grijspeerdt et al [41]. To make a selection of these models, the simulation results from each model were fitted to the measured data collected in a downscale decanter. An advanced approach called *a posteriori* technique selecting models on the basis of certain parameter invariant characteristics of the models was introduced to fit the model results and observations. Four major selection

criterions were:

1. The goodness of model fit.

2. The complexity of the model.

3. The level of difficulty of estimating the parameters.

4. The ability to develop unique model parameters based on the available data sets.

The steady-state fitting results showed that both Takács's 10-layer model and Hamilton's dispersion model provided a better model fit compared with other models. The dispersion model took less time to calculate the parameters, because it only contained three parameters as opposed to five parameters needed in the 10-layer model. However, the dispersion model failed to pass the cross-validation test, because the dispersion term *D* was too sensitive to various operation conditions, and ranged widely for different datasets. Under dynamic simulation condition, the 10-layer model results also fitted the real measured data sets better than others, but still took longer time for parameter estimation [41].

For a well known reason that the short-circuiting and the density current greatly impact the settling behavior in the thickener, Dupont and Dahl proposed a special dynamic model to simulate both phenomena. The strategy to deal with the short-circuiting was to add a short-circuiting factor Ω, a simple dilution factor, which can be calculated by forming a simple mass conservation equation for thickener [42]. The density current

problem can be handled by adjusting the height of the inlet according to the feed flow solids concentration. Plósz [43] utilized the same strategy to simulate the density current, and indicated that the maximum height of the feed layer should be restricted to 53% of the clarifier height. In a fashion similar to Otterpohl's previous work [39], Dupont and Dahl divided the components of influent solids into three categories: soluble components, primary particles unable to settle, macroflocs able to settle. They proposed that the concentration of primary particles in the influent flow be described as the following equation 14:

$$X_{PP} = SS_{\inf} + K_1 \cdot \left(\frac{Q_{efl}}{A} \right)^{K_2} \tag{14}$$

So the concentration of macroflocs can be expressed as:

$$X_{ss} = X_{ss,j} - X_{pp} \tag{15}$$

The settling velocity of macroflocs was determined by an original equation as follow:

$$V_s = V_0 \cdot \exp\left\{ -0.5 \cdot \left[\frac{\ln\left(\frac{X_{ss} + X_{pp}}{n_1} \right)}{n_2} \right] \right\} \tag{16}$$

The simulation results indicated that it was possible to set up a one-dimensional model including both of the short-circuiting and density current. This model can predict the solids concentration profile through

the thickener and the effluent solids concentration very well. More investigations were required to investigate the relationship between the short-circuiting factor and other parameters.

One remaining problem of one-dimensional clarifier model was that the concentration profile based on the analytical solutions was sensitive to the number of model layers, as discussed in Hamilton's paper[37]. One possible reason causing this problem was the numerical methods used in solving these partial differential equations were not accurate enough. Jeppsson and Diehl proposed a new numerical method called Godunov flux [44].

Another significant adjustment of the traditional dynamic model was the boundary condition. Instead of prescribing a boundary condition that the effluent and underflow solids concentration are same as the concentration within the settler at the bottom and top, Jeppsson and Diehl stated that the only correct boundary condition was the conservation law. A source term was also added to the traditional partial differential equation. The well-known 10-layer model was selected for comparsion, because of the confirmed validity confirmed by Grijspeerdt [41]. The comparison showed that the Jeppsson and Diehl was not sensitive to the number of layers, and the solids profile more closely resembled the ideal concentrations calculated from inventory models such as Tracy's[3]. Jeppsson and Diehl also recommended that 30 layers as the lower limit to guarantee reliable simulation results under normal operation conditions[44]. Jeppsson and Diehl[44] noted that their results tended to

be mathematically elegant solutions rather than real predicted values for practical application.

Noticing that the main drawback of Takács's constraint model and Hamilton's dispersion model was the layer's number *n* became a parameter and seriously affected the simulation results, David et al. proposed a new numerical approach called method of lines (MOL) with different boundary conditions to solve the dispersion model[45]. His method was different from the traditional up-wind schemes and implicit boundary condition. His solution proceeded in two steps:

1. Spatial derivatives are first approximated using, for instance, finite-difference methods.

2. The resulting system of semi-discrete (discrete in space but still continuous in time) equations is integrated in time.

The new boundary conditions were as equation 17 and 18:

$$V_{s,i} \cdot C_1 - D_1 \cdot \frac{\partial C_i}{\partial Z_i} = 0 \qquad \text{(top and bottom layer)} \qquad (17)$$

$$C_i = \frac{q_f \cdot C_f}{q_e + q_u} \qquad \text{(feed layer)} \qquad (18)$$

The simulating result of the Hamilton's dispersion model with different numbers of layers showed that the application of MOL and the new boundary condition can provide numerical solutions insensitive to the layers' number. Another sound advantage of the application of the MOL

and the new boundary condition was that the model was able to be implemented in a MATLAB simulator conveniently [45]. In accordance with Jeppsson and Diehl's conclusion, David also suggested that increasing the number of model layers can improve the numerical accuracy of the solids concentration profiles[45].

Though both Takács's 10-layer model and Hamilton's dispersion model provide reliable predictions of the solids concentration profile, the possible correlation between them still remains unknown. Watts et al. illustrated that the function of Stenstrom's gravity flux constraint was equivalent to adding a solids concentration and layer's thickness dependent dispersion term as shown in equation 19 to the original discretization equation[46].

$$D_{i,i+1} = \delta Z \cdot \frac{-\partial G_s}{\partial C} \tag{19}$$

In equation 19 the dispersion coefficient disappears as the layer thickness δZ approaches zero, which was not physically plausible. Therefore Watts' modified equation 20, where α is a constant as follows:

$$D_{i,i+1} = \alpha \cdot \frac{-\partial G_s}{\partial C} \tag{20}$$

The dispersion term D was no longer sensitive to the layers' thickness [46]. A special threshold concentration was introduced as $C_{crit} = 2/b$, ($b=r_h$, r_h is one parameter in Takács's settling velocity equation). The dispersion coefficient equaled to D_{max}, a function dependent on the feed flow velocity,

when the solids concentration was larger than C_{crit}; otherwise it can be calculated by equation 20.

A new dynamic clarifier model was proposed by Clercq et al.[47]. The special characteristic of this model was that it included a two flow rate dependent dispersion term in clarification zone and thickening zone respectively.

$$D_1(t) = D_{11} * e^{\alpha \cdot \frac{Q_e(t)}{Q_f(t)}} \qquad D_2(t) = D_{22} * e^{\beta \cdot \frac{Q_u(t)}{Q_f(t)}} \qquad (21, 22)$$

Where the D_{11}, D_{22}, α and β are the dispersion parameters that need to be calibrated, but for a specific clarifier, these parameters are constants [47]. The model also included a height-dependent cross sectional area, which was similar to Laikari's strategy. Excellent descriptive capabilities were obtained for sludge profiles and sludge blanket height, but not for the effluent solids concentration, due to the poor quality measurements at the surface of the clarifier [47].

Plósz et al. conducted a further investigation of the dispersion coefficient, and confirmed that the dispersion coefficient should not be only governed by the feed flow, but also by other factors, as the outflow velocities, as also noted by Clercq et al[43]. They also showed that Watts' exponential approach to determine the dispersion coefficient can not work under the condition R ($R=V_{un}/V_f$) $\geqq 0.45$, and Clercq's idea that two different dispersion terms in clarification zone and thickening zone always gave a over-predication in high concentration zone and under-predication in the

low concentration zone [48]. Instead of being a function of the feed flow velocity, the dispersion coefficient in this model was expressed as a function related to the overflow rate. Other adjustments of the traditional dispersion model were the addition of a feed flow dependent reduction factor into the downward convection term μ to improve the simulation accuracy in the thickening zone, and the suction-lift sludge removal system was simulated by an array of fluxes, withdrawing sludge not only from the last but from several other layers up to the height of the suction collector. This clarifier model can provide an improved assessment of the clarifier storage capacity and the sludge concentration in the effluent flow [43].

Most of the available dynamic models were derived based on the empirical equations, however these empirical equations had no relationship with the physical properties of the activated sludge flocs and solid-water interaction [49]. Clercq provided a new mechanistic model based on the conservation law of mass and momentum. This model included a Kynch batch density function $f_{bk}(C)$ and an effective solids stress $\sigma_e(C)$ as shown in equation 24. The gravity settling velocity in the hindered zone was described by the Cho equation, and equation 23 was used to express the gravity settling velocity in the compression zone.

$$V_s = \frac{f_{bk}}{C}\left(1 - \frac{\rho_s}{\Delta\rho \cdot g \cdot C} \cdot \frac{\partial \sigma_e}{\partial z} \cdot \frac{\partial C}{\partial z}\right) \tag{23}$$

$$\frac{\partial C}{\partial t} = -\frac{\partial f_{bk}}{\partial z} + \frac{\partial}{\partial z}\left(f_{bk}(C)\frac{\rho_s}{\Delta\rho \cdot g \cdot C} \cdot \frac{\partial \sigma_e}{\partial z} \cdot \frac{\partial C}{\partial z}\right) \tag{24}$$

Where C = solids concentration; t = time; z = depth in settling column; f_{bk} = Kynch batch density function; ρ_s = solids mass density; g = gravity constant; σ_e = effective solids stress as shown in equation 25:

$$\sigma_e = \alpha \cdot \ln\left(\frac{C - C_C + \beta}{\beta}\right) \tag{25}$$

Where α and β = calibration parameters, C_c = the compression solids concentration, defined as the concentration at which the concentration gradient reaches the values below 200g/l/m within the sludge blanket. The numerical method used up-wind differencing for the first-order term and central differencing for the secondary-order term. The batch tests indicated that this model can describe the settling behavior significantly better than any other model [49].

To build consensus on a constant modeling methodology (CMM), Bürger et al drew a comprehensive conclusion of previous works and separated the model building process into six steps as follow:

1. Construction of a mathematical model on the basis of physical law;

2. Estimate well-posedness;

3. Numerical method and simulation program;

4. Calibration;

5. Validation;

6. Rebuilding or extension of the model;

The key principles of the CMM was that for a real process that occurs in a continuous time and space, the modeling should be done in continuous time and space, resulting in a PDE as mathematical model, and the parameters should never be introduced into the simulation model directly [50].

Following the six steps in CMM, Bürger et al built a robust dynamic model which included most of the previously described physical phenomena as hindered settling, compression and dispersion. They believed that time has come to incorporate established mathematical techniques into environment engineering, and waste water modeling in particular, and to use proven reliable and consistent simulation models [50].

3. RESULTS AND DISCUSSION

3.1. Original Dynamic Settling Model

3.1.1. Rebuilding the Original Dynamic Settling Model

To proceed to establish a dynamic secondary clarifier model, it is necessary to make several assumptions in order to create a solvable mathematical problem. The following assumptions are made:

1. The clarifier is circular and central-feed.

2. No density currents happen in the clarifier.

3. The biochemical reaction rate approaches to zero in the clarifier.

4. Uniform loading rate neglecting any wild influence.

5. Mechanical sludge scraper does not affect the sludge settling behavior.

6. Wall effects can be ignored.

The secondary clarifier can be divided into several vertical layers. For each layer, the following assumptions are made to simulate the settling behavior without knowing the specific forces acting on the particles.

7. The area and the thickness of each layer are fixed.

8. Incoming solids are distributed instantaneously and uniformly in the

feed layer.

9. The settling velocity is function only related to the solids concentration in the specific layer.

10. The gravity settling flux in the bottom layer is zero, since it is a physical boundary of the clarifier.

11. The dispersion flux is zero (plug flow).

Based on flux theory, a mass conservation can be defined for layer ***i***:

$$Accumulation = Input - Output \pm Reaction \quad (26)$$

Since the Reaction term equals to zero, according to the assumption that there are no biochemical reactions in the clarifier, equation 26 can be simplified as:

$$Accumulation = Input - Output \quad (27)$$

So for the layer above the inlet, containing the feed point and below the feed point, equations can be expressed as equation 28, 29, 30:

$$V\frac{dC}{dt} = A\cdot\left(v_{i-1}\cdot C_{i-1} - v_i\cdot C_i\right) + A\cdot\left(u_o\cdot C_{i+1} - u_o\cdot C_i\right) \quad \text{(clarification zone)} \quad (28)$$

$$V\frac{dC}{dt} = A\cdot\left(v_{i-1}\cdot C_{i-1} - v_i\cdot C_i\right) - A\cdot\left(u_o\cdot C_i + u_u\cdot C_i\right) + A\cdot\left(u_o + u_u\right)\cdot MLSS$$

(feed point) (29)

$$V\frac{dC}{dt} = A\cdot\left(v_{i-1}\cdot C_{i-1} - v_i\cdot C_i\right) + A\cdot\left(u_u\cdot C_{i-1} - u_u\cdot C_i\right) \qquad \text{(thickening zone)} \quad (30)$$

Where V= volume of every layer; A=the area of every layer; v_i=the gravity settling velocity in layer i; C_i=the solids concentration in layer i; u_o=the overflow rate; u_u=the underflow rate; $MLSS$=the initial feed solids concentration.

Since a layer volume is the product of layer area and thickness ($V=A\cdot dZ$), dz is the thickness of each layer, equation 28, 29, 30 can be transformed as follows:

$$\frac{dC}{dt} = \frac{\left(v_{i-1}\cdot C_{i-1} - v_i\cdot C_i\right)}{dz} + \frac{\left(u_o\cdot C_{i+1} - u_o\cdot C_i\right)}{dz} \qquad \text{(clarification zone)} \quad (31)$$

$$\frac{dC}{dt} = \frac{\left(v_{i-1}\cdot C_{i-1} - v_i\cdot C_i\right)}{dz} - \frac{\left(u_o\cdot C_i + u_u\cdot C_i\right)}{dz} + \frac{\left(u_o + u_u\right)}{dz}\cdot MLSS \qquad \text{(feed point)} \quad (32)$$

$$\frac{dC}{dt} = \frac{\left(v_{i-1}\cdot C_{i-1} - v_i\cdot C_i\right)}{dz} + \frac{\left(u_u\cdot C_{i-1} - u_u\cdot C_i\right)}{dz} \qquad \text{(thickening zone)} \quad (33)$$

Recalling the definition of the flux theory, $V_i{\cdot}C_i$ can be defined as the gravity settling flux G_s:

$$\frac{dC}{dt} = \frac{dG_s}{dz} + \frac{u_o\cdot dC}{dz} \qquad \text{(clarification zone)} \quad (34)$$

$$\frac{dC}{dt} = \frac{dG_s}{dz} - \frac{\left(u_o\cdot C_i + u_u\cdot C_i\right)}{dz} + \frac{\left(u_o + u_u\right)}{dz}\cdot MLSS \qquad \text{(feed point)} \quad (35)$$

$$\frac{dC}{dt} = \frac{dG_s}{dz} + \frac{u_u\cdot dC}{dz} \qquad \text{(thickening zone)} \quad (36)$$

By letting the finite difference operators approach zero, a first-order partial differential equation can be derived to describe the continuous settling process in the secondary clarifier.

$$\frac{\partial C(z,t)}{\partial t}+\frac{\partial G_s(C(z,t))}{\partial z}+u\frac{\partial C(z,t)}{\partial z}=s(t)\delta(z) \tag{37}$$

Where u stands for the flow rate, $u=u_o$ in the clarification zone, $u=u_u$ in the thickening zone; $s(t)\delta(z)$ is a source term and $\delta(z)$ is the delta function, equal to one when z=height of the feed point, otherwise, $\delta(z)$ equals to zero.

3.1.2. Simulation of the Underloading and Overloading Conditions

According to assumption 9 that the gravity settling velocity is determined by the solids concentration, two previously-defined equations can be used: Vesilind equation 39 [36]and Takács et al equation 38[2].

$$\begin{cases} V_{sj}=V_0\cdot e^{r_h\cdot X^*_j}-V_0\cdot e^{r_p\cdot X^*_j} \\ 0\le V_{sj}\le V_0^{'}\le V_0 \end{cases} \tag{38}$$

$$V_{sj}=V_0\cdot e^{-b\cdot c} \tag{39}$$

Li and Ganczarczyk showed that the Vesilind equation can only be applied to the hindered settling condition, which means it probably can not adequately describe the gravity settling velocity in the clarification zone[51]. Finally, Takács equation is selected in this study for an accuracy issue. Data for the simulated WWT plant are given in the Table.1 [44].

Table 1- Data for the simulated WWT plant

Settling Velocity Parameters		
V_0	6.04	m/h
V_0'	4.17	m/h
r_p	0.005	m^3/g
r_h	0.00042	m^3/g
X_{min}	10	mg/l
Design and operational variables		
Settler surface area	500	m^3
Settler depth	4	M
Settler inlet depth	1.8	m
Influent flow rate	250	m^3/h
Recycle flow rate	200	m^3/h
Dispersion term	0.542	m^2/h

The double exponential Figure 1 describing the evolution of the gravity settling velocity includes five parameters as discussed in the literature review, and their functions are also shown in Figure 1. So the gravity settling flux G_s ($G_s=v_s \cdot C$) under different solids concentration conditions can be calculated from the relations in Figure 1, as shown in Figure 2.

Figure 2 is the gravity settling flux, and shows that in the low concentration domain, the gravity settling flux increases with concentration, but decreases as the concentration grows in the high concentration domain. There always exists a peak gravity settling flux for the slurries with specific subsidence characteristics.

Yoshioka [25] showed that the gravity settling flux can be utilized to determine the limiting flux, the maximum flux that can be conveyed to the bottom of the thickener without causing a sludge blanket rise. However, Yoshioka's method is not so explicit as Hassett's strategy of determining the limiting flux upon a total flux figure (total flux= gravity settling flux + bulk flux) [26]. Both methods when applied correct yield the same result. The limiting flux in this study is determined by Hasset's total flux method as shown in Figure 3.

Based on Hassett's theory that the minimum point governs the solids handling capacity of the thickener, and a line tangent to the minimum point intercepts the ordinate at the limiting flux, the limiting flux of the simulated thickener is 4844.8 g/m^3-h, meanwhile, the intersection of this tangent line with the bulk flux curve dictates the maximum recycle solids concentration C_r=12112 g/m^3. Simulation results are presented with more

significant figures that warranted for a physical clarifier, but are provided to document the actual simulation results, should a reader want to reproduce them.

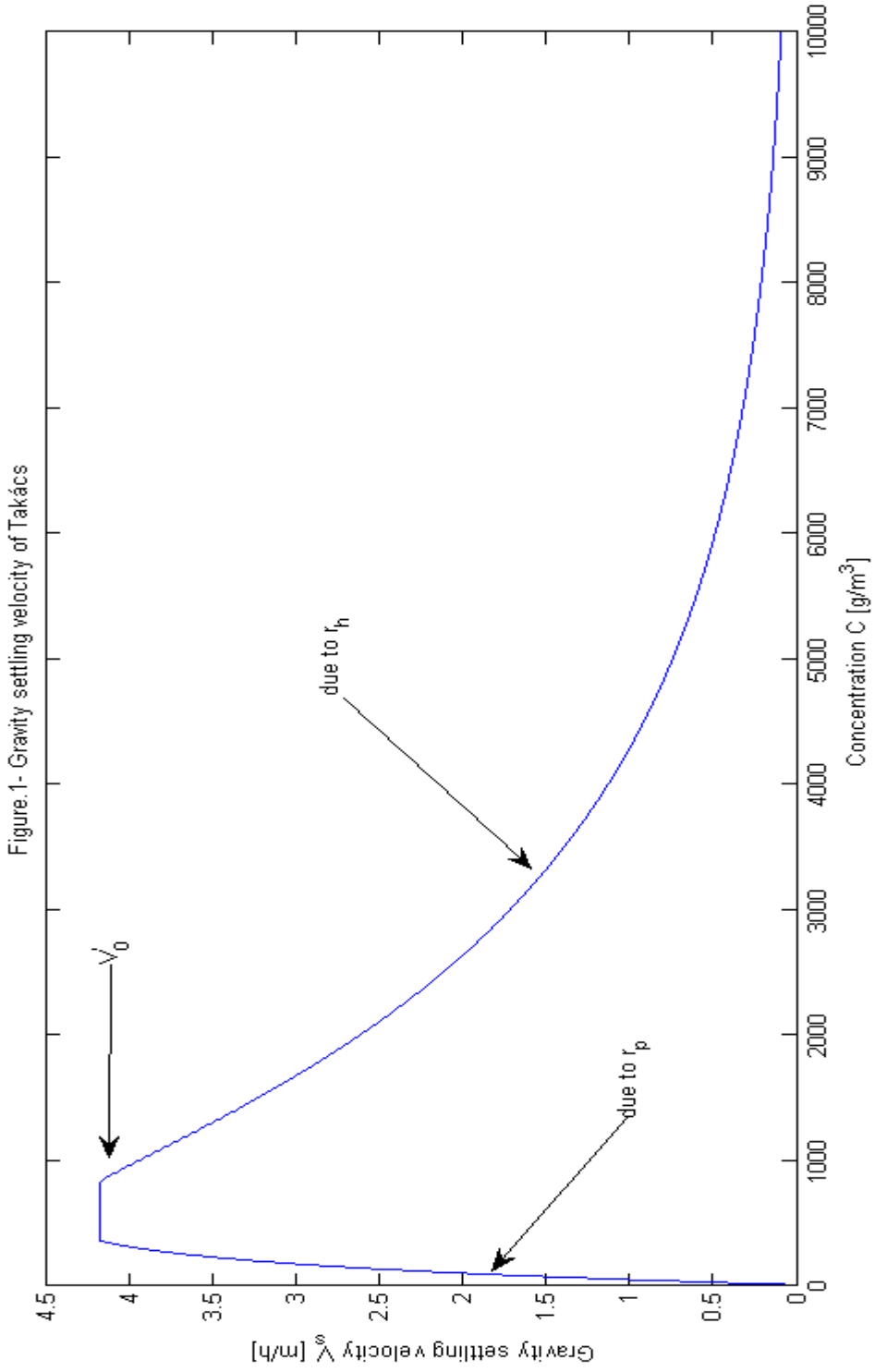
Figure.1- Gravity settling velocity of Takács
Gravity settling velocity V_g [m/h]
Concentration C [g/m^3]
V_0'
due to r_h
due to r_p
0
0.5
1
1.5
2
2.5
3
3.5
4
4.5
0
1000
2000
3000
4000
5000
6000
7000
8000
9000
10000

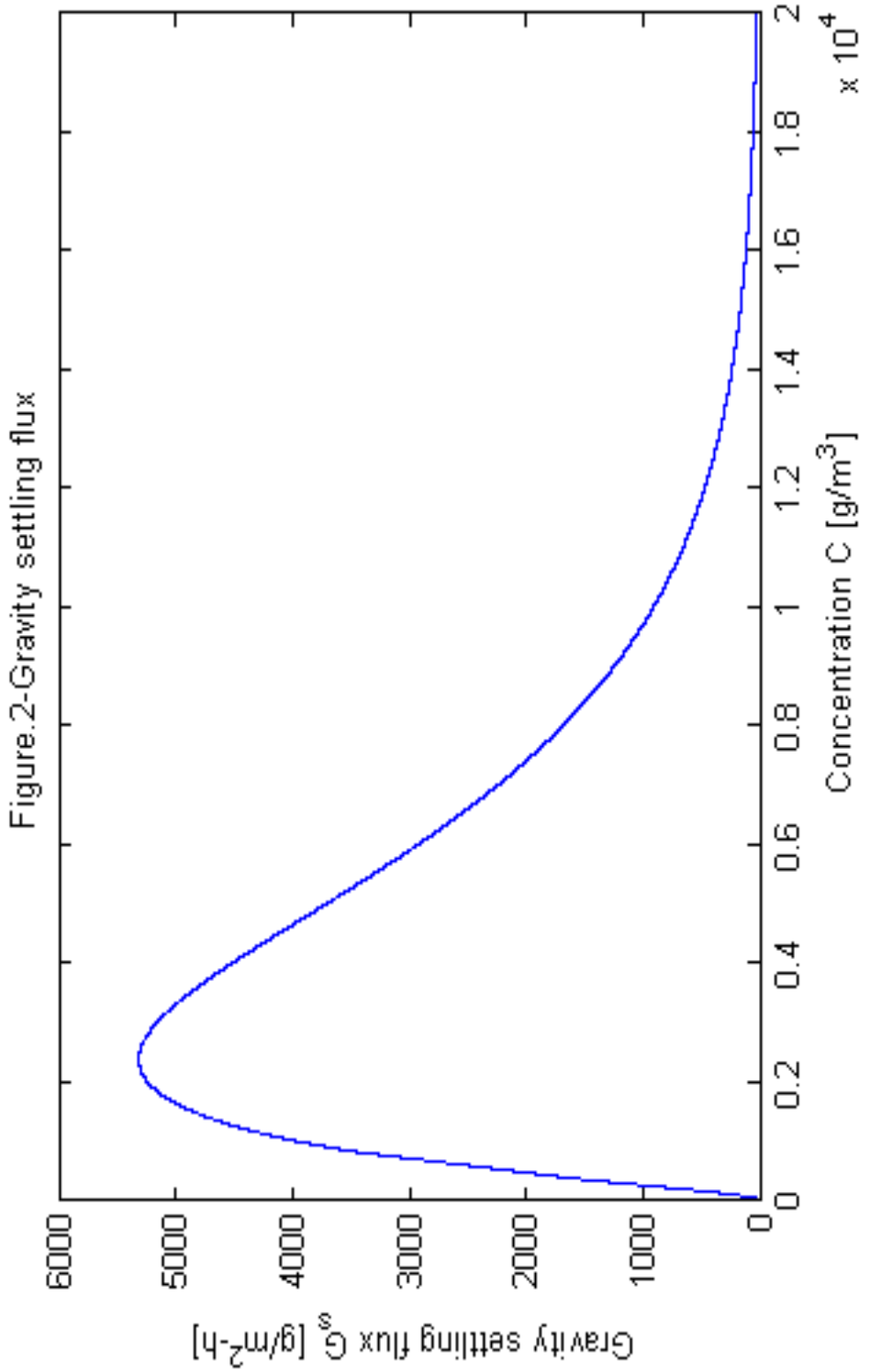
Figure.2-Gravity settling flux
Gravity settling flux G_s [g/m^2-h]
Concentration C [g/m^3]
x 10^4
0
1000
2000
3000
4000
5000
6000
0
0.2
0.4
0.6
0.8
1
1.2
1.4
1.6
1.8
2

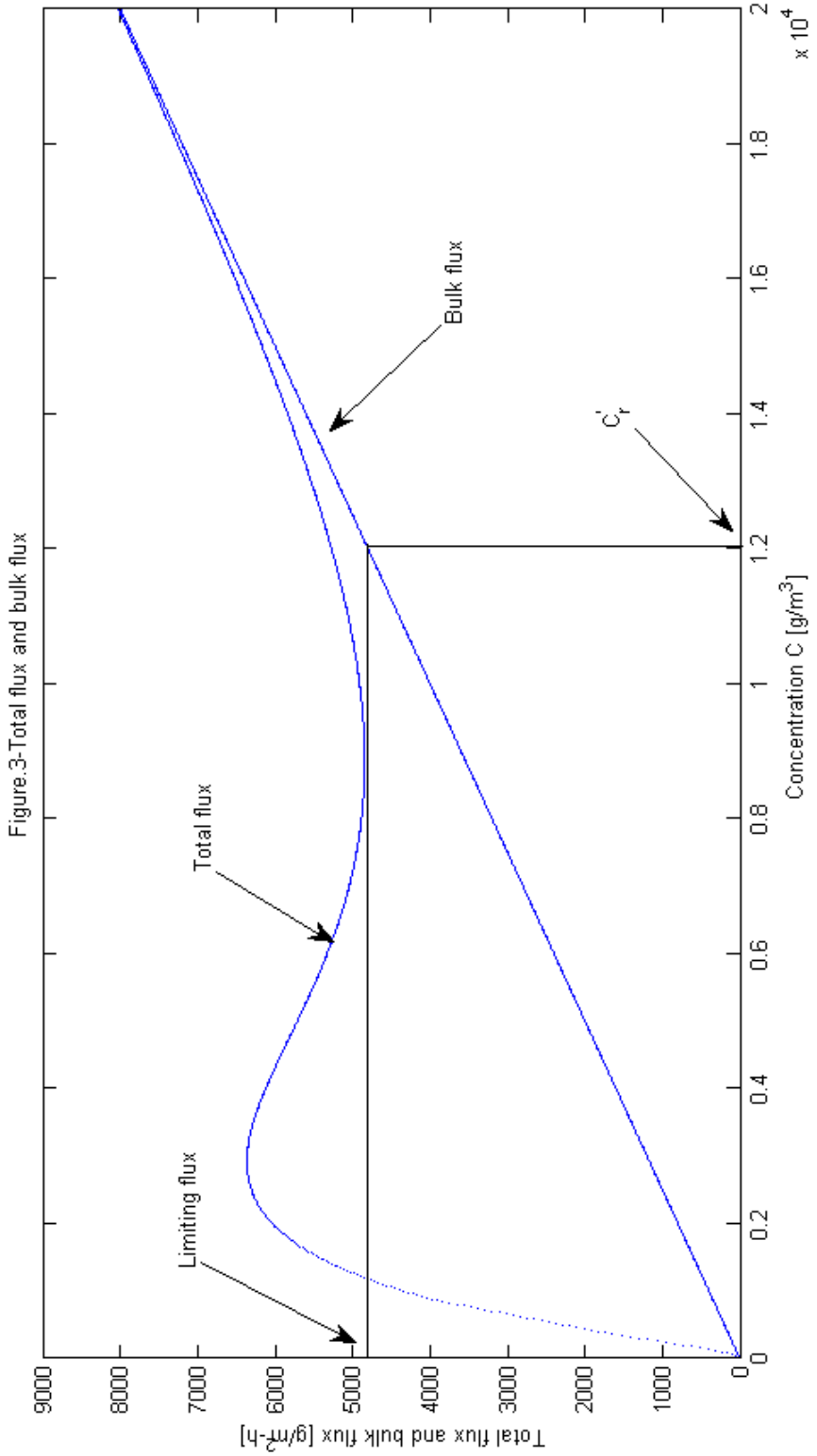
Figure.3-Total flux and bulk flux
Total flux and bulk flux [g/m²-h]
Concentration C [g/m³]
x 10⁴
Limiting flux
Total flux
Bulk flux
C'r
0
1000
2000
3000
4000
5000
6000
7000
8000
9000
0.2
0.4
0.6
0.8
1
1.2
1.4
1.6
1.8
2

The numerical method to solve equation 37 is the first-order up-wind scheme, and the analogs are given as follow:

$$\frac{\partial C}{\partial t} = \frac{C_i^{n+1} - C_i^n}{\Delta t} \tag{40}$$

$$\frac{\partial G}{\partial z} = \frac{G_i^n - G_i^{n-1}}{\Delta t} \tag{41}$$

$$\begin{cases} \dfrac{\partial C}{\partial z} = \dfrac{C_i^n - C_{i-1}^n}{\Delta z} & \text{Clarification zone} \quad (42) \\ \dfrac{\partial C}{\partial z} = \dfrac{C_i^n - C_{i+1}^n}{\Delta z} & \text{Thickening zone} \quad (43) \end{cases}$$

To completely test the accuracy and feasibility of the original dynamic model, the model is used to simulate two different loading conditions: underloading condition which means the operation flux is smaller than the limiting flux, and overloading condition which means the operation flux is larger than the limiting flux.

In order to obtain a steady-state underloading condition, which means the effluent solids concentration and the underflow solids concentration do not change with time, the MLSS and simulation time interval are fixed at 5000 g/m^3 (the operation flux=4500 g/m^3-h<the limiting flux) and 20 hours. The initial concentration C(x,0)=0.

Figure 4 is the calculated solids concentration profile at 20 h, and Figure 5 is a dynamic solids concentration profile simulated from 0 to 20 h. Figure 5 shows that the clarifier reaches steady-state in less than one hour. Figure 4 presents the evaluated underflow solids concentration C_r=11234

g/m^3, similar to the predicted value 11250 g/m^3, and the effluent solids concentration C_e= 11.06 g/m^3.

Under an overloading condition, the MLSS and simulation time interval are fixed at 6000 g/m^3 (the operation flux=5400 g/m^3-h>the limiting flux) and 20 hours. The initial concentration C(x,0)=0.

Under an overloading condition, a continuous sludge blanket rise can be observed until the sludge blanket level exceeds the clarifier effluent weir, resulting in sludge waste. However, the dynamic simulation results in Figure 7 shows that a steady state can still be observed under an overloading condition, similar to what happens in the underloading case. Another contradiction is that the underflow solids concentration C_r predicted in Figure 6 is 13484 g/m^3, much larger than the possible maximum underflow solids concentration $C_r^{'}$=12112 g/m^3, predicted in Figure 3 upon the basis of flux theory and Hassett method.

As a conclusion, the original dynamic (no constraint on flux) model can exactly predict the solids concentration profile, as well as the effluent and underflow solids concentration in an underloading situation. Nevertheless, for an overloading condition, the original model fails in predicting the rise of sludge blanket height and underflow solids concentration. The piratical application value of this model deteriorates seriously, due to these obvious drawbacks. Bryant noted this back in 1972.

Figure.4 Solids concentration profile

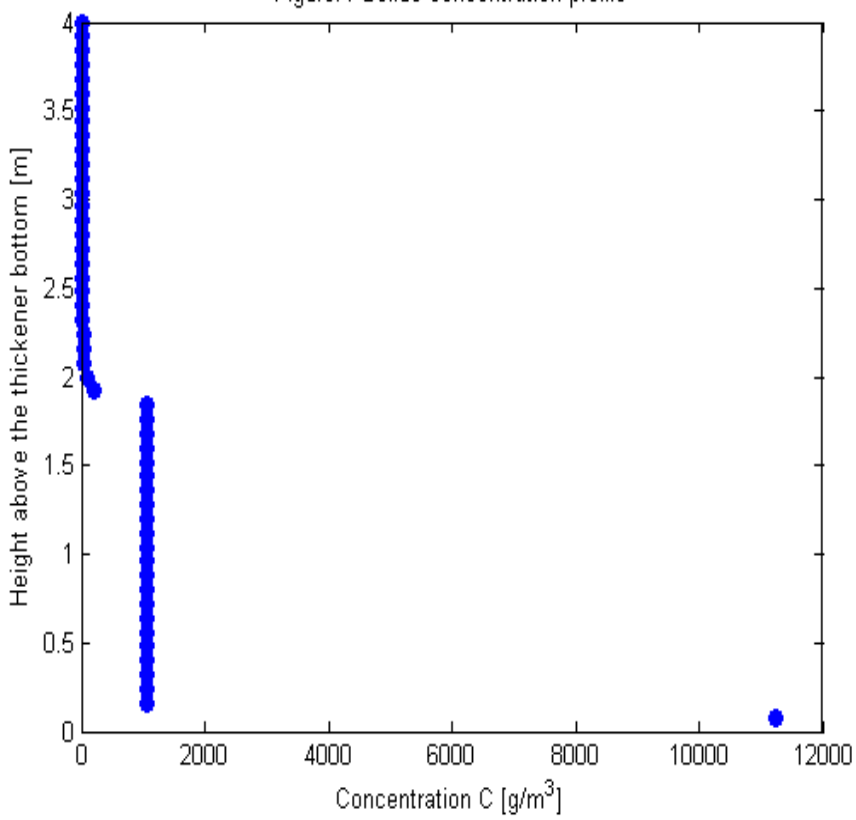

Figure.5 A dynamic solids concentration profile as a function of time and height

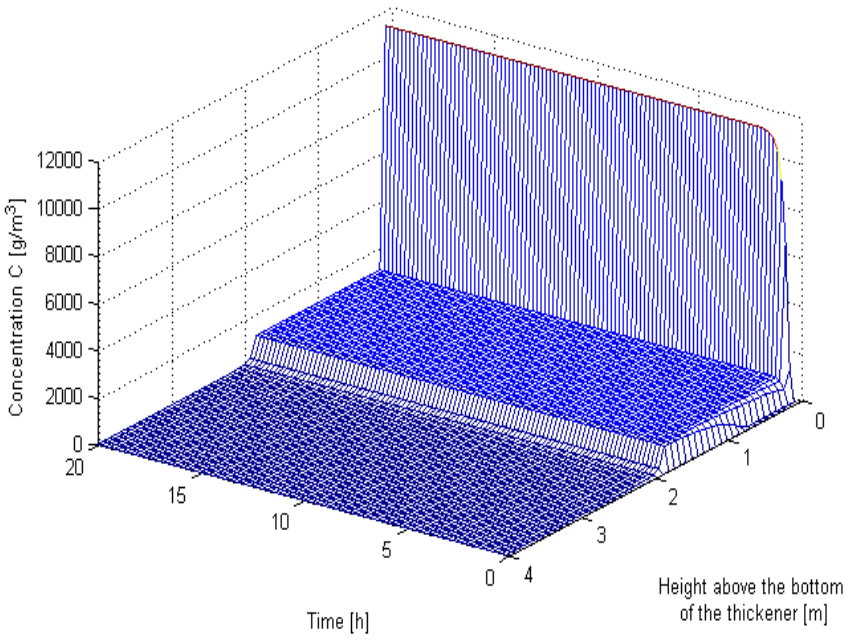

Figure.6- Solids concentration profile

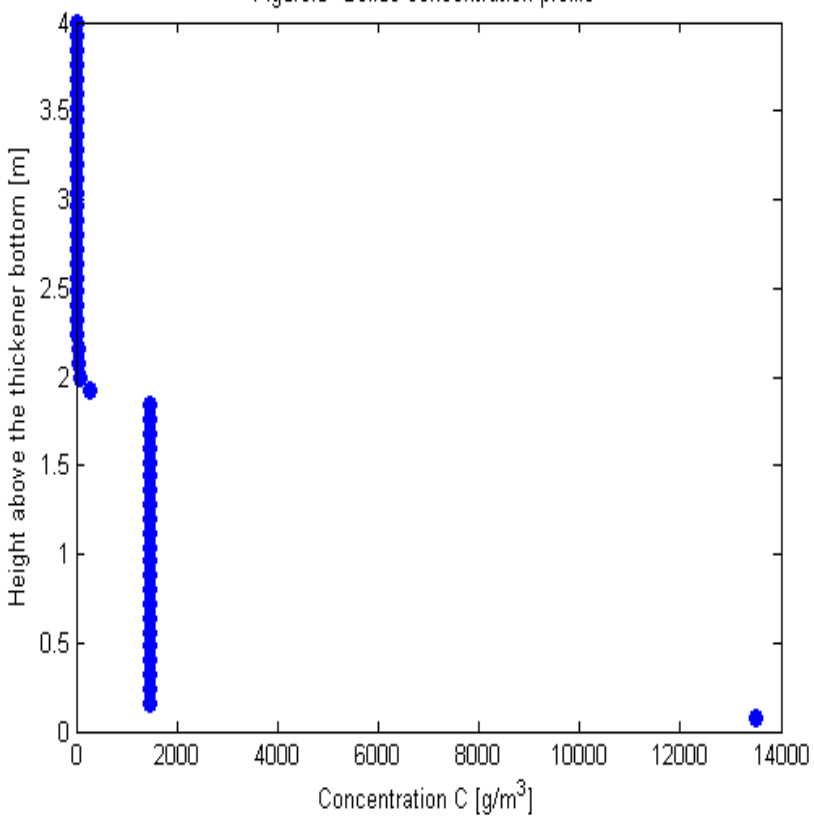

Figure. 7- A dynamic solids concentration profile as a function of time and height

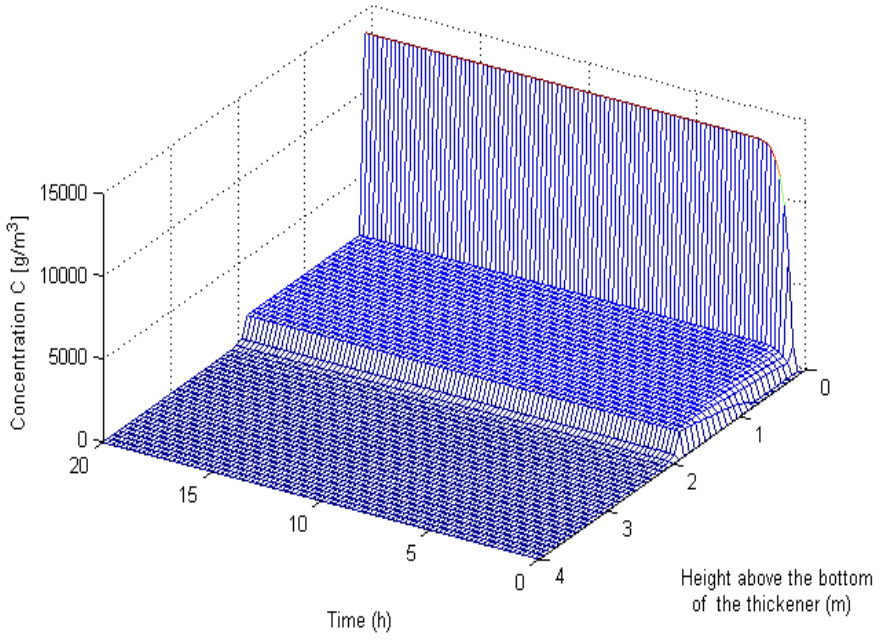

3.2. Modification of the Original Dynamic Model

3.2.1. Gravity Flux Constraint Model and Dispersion Model

As supplements of the original dynamic model, several approaches have been developed to enhance the initial dynamic model's reliability in overloading condition. Based on a comprehensive analysis of various factors, including fitting results, the complexity of the improved model, the difficulty level to calculate modeling parameters, two of them Stenstrom's gravity settling flux constraint and Hamilton's dispersion term, have been demonstrated to be most effective, confirmed by Grijspeerdt [33, 37, 41].

To deal with the deterioration in overloading condition, the strategy developed by Stenstrom was to add an extra assumption to impose a special restriction on the gravity settling flux: the mass flux into a differential volume can never exceed the flux which the volume is capable of passing nor can it exceed the flux which the next higher differential volume is capable of transmitting[33]. Therefore the gravity flux constraint model is expressed with the following up-wind scheme:

$$\frac{C_i^{n+1}-C_i^n}{\Delta t}=-u_o\frac{\left(C_i^n-C_{i+1}^n\right)}{\Delta z}-\frac{\left(\min\left(G_i^n,G_{i+1}^n\right)-\min\left(G_i^n,G_{i-1}^n\right)\right)}{\Delta z} \quad (44)$$

$$\frac{C_i^{n+1}-C_i^n}{\Delta t}=-\frac{\left(\min\left(G_i^n,G_{i+1}^n\right)-\min\left(G_i^n,G_{i-1}^n\right)\right)}{\Delta z}-\frac{\left(u_o\cdot C_i+u_u\cdot C_i\right)}{\Delta z}+\frac{\left(u_o+u_u\right)}{\Delta z}\cdot MLSS \quad (45)$$

$$\frac{C_i^{n+1}-C_i^n}{\Delta t}=-u_u\frac{\left(C_i^n-C_{i\text{-}1}^n\right)}{\Delta z}-\frac{\left(\min\left(G_i^n,G_{i+1}^n\right)-\min\left(G_i^n,G_{i-1}^n\right)\right)}{\Delta z} \quad (46)$$

In Hamilton's dispersion equation, the addition of an effective dispersion term provides an extra mixing effect, and converts the original first-order hyperbolic partial differential equation to a second-order parabolic partial differential equation by adding a second-order derivative.

$$\frac{\partial C(z,t)}{\partial t}+\frac{\partial G_s(C(z,t))}{\partial z}+u\frac{\partial C(z,t)}{\partial z}-\mathrm{D}\frac{\partial^2 C(z,t)}{\partial z^2}=s(t)\delta(z) \quad (47)$$

The up-wind differencing is used for the first-order time and spatial terms, same as the analogs used in the original model. Conservative discretisation of the secondary-order spatial term is achieved by using the following second-order analog, so the Hamilton dispersion model can be discretized as follows:

$$\frac{\partial^2 C}{\partial z^2}=\frac{C_{i+1}^n-2C_i^n+C_{i-1}^n}{\Delta z^2} \quad (48)$$

$$\frac{C_i^{n+1}-C_i^n}{\Delta t}=-u_o\frac{\left(C_i^n-C_{i+1}^n\right)}{\Delta z}-\frac{\left(G_i^n-G_{i-1}^n\right)}{\Delta z}+D\frac{\left(C_{i+1}^n-2\cdot C_i^n+C_{i-1}^n\right)}{\Delta z^2} \quad (49)$$

$$\frac{C_i^{n+1}-C_i^n}{\Delta t}=-\left(\frac{G_i^n-G_{i-1}^n}{\Delta z}\right)-\frac{\left(u_o\cdot C_i+u_u\cdot C_i\right)}{\Delta z}+\frac{\left(u_o+u_u\right)}{\Delta z}\cdot MLSS+D\frac{\left(C_{i+1}^n-2\cdot C_i^n+C_{i-1}^n\right)}{\Delta z^2}$$

(50)

$$\frac{C_i^{n+1}-C_i^n}{\Delta t}=-u_o\frac{\left(C_i^n-C_{i-1}^n\right)}{\Delta z}-\frac{\left(G_i^n-G_{i-1}^n\right)}{\Delta z}+D\frac{\left(C_{i+1}^n-2\cdot C_i^n+C_{i-1}^n\right)}{\Delta z^2} \quad (51)$$

3.2.2. Simulation of the Underloading and Overloading Conditions

Both the gravity flux constraint model and dispersion have been employed to simulate the underloading and overloading situation respectively, for the purpose to verify possible improvements in predication.

The underloading operation parameters are the same as those used in the original model simulation: the MLSS and simulation time interval are fixed at 5000 g/m^3 (the operation flux = 4500 g/m^3-h<the limiting flux) and 20 hours. The initial concentration C(x,0) = 0.

Based on the gravity flux constraint model, Figure 8 shows the calculated solids concentration profile at 20 h, and Figure 9 is a dynamic solids concentration profile from 0 to 20 h. Figure 9 shows that a stead state situation can be attained in less than one hour, similar to the original model estimation. Figure 8 presents the calculated underflow solids concentration C_r = 11238 g/m^3, similar to the predicted value 11250 g/m^3, and the effluent solids concentration C_e = 11.14 g/m^3. Both Figures 8 and 9 illustrate the gravity flux constraint model can succeed in predicting the existence of compression zone, the huge concentration gradient occurring near the thickener bottom, which matches the actual observation results in both batch and continuous settlings, while the original model fails in predicting the existence of compression zone.

Based on the dispersion model, Figure 10 shows the calculated solids concentration profile at 20 h, and Figure 11 is a dynamic solids

concentration profile from 0 to 20 h. The Figure 11 shows that the dispersion model illustrates a sludge blanket rise which is inexistent under an underloading condition. Figure 10 presents the evaluated underflow solids concentration C_r = 9578 g/m^3, much smaller than the predicted value 11250 g/m^3. Consequently, both Figures 10 and 11 indicate the dispersion model fails in predicting the solids concentration profile and the underflow solids concentration in an underloading situation.

For the purpose of comparing simulations, the same parameters are used in an overloading situation: the MLSS and simulation time interval are fixed at 6000 g/m^3 (the operation flux = 4500 g/m^3-h<the limiting flux) and 20 hours. The initial concentration C(x,0) = 0.

The dynamic simulation results in Figure 13 shows that a sludge blanket rise occurs under an overloading condition, which matches the observation in both batch and continuous settling processes. Therefore the gravity flux constraint model can work well in predicting the sludge blanket height rise, while the original model can not. The underflow solids concentration C_r evaluated in Figure 12 is 11974 g/m^3, similar to the theoretically maximum recycle solids concentration C'_r = 12112 g/m^3, predicted in Figure 3 on the basis of flux theory and Hassett method.

Figure 15 shows that the dispersion model can also predict the sludge blanket rise under an overloading condition. But the predicted sludge blanket rise rate from the gravity flux constraint model and the dispersion model are not similar: the rise rate observed from dispersion model is mush faster than the one from gravity flux constraint model. The sludge

blanket height has exceeded the effluent weir in Figure 15, while Figure 13 shows that it is only above the feed point within the same time interval. The underflow solids concentration C_r evaluated in Figure 14 is 9986g/m^3, much smaller than the theoretically maximum recycle solids concentration C'_r = 12112 g/m^3, predicted in Figure 3 on the basis of flux theory and Hassett method. So, in an overloading situation, the dispersion model can succeed in predicting the rise of sludge blanket, but underflow solids concentration evaluation still remains inaccurate.

In conclusion, either of the gravity flux constraint model and the dispersion model can evaluate the sludge blanket rise in an overloading condition, though the predicted rise rates are different. In addition to estimating the sludge blanket rise, the gravity flux control model can work well in evaluating the underflow solids concentration in both underloading and overloading situations, while the dispersion model can not give accurate underflow concentration predication in both situations.

Figure.8-Solids concentration profile
(Gravity flux constrain model)

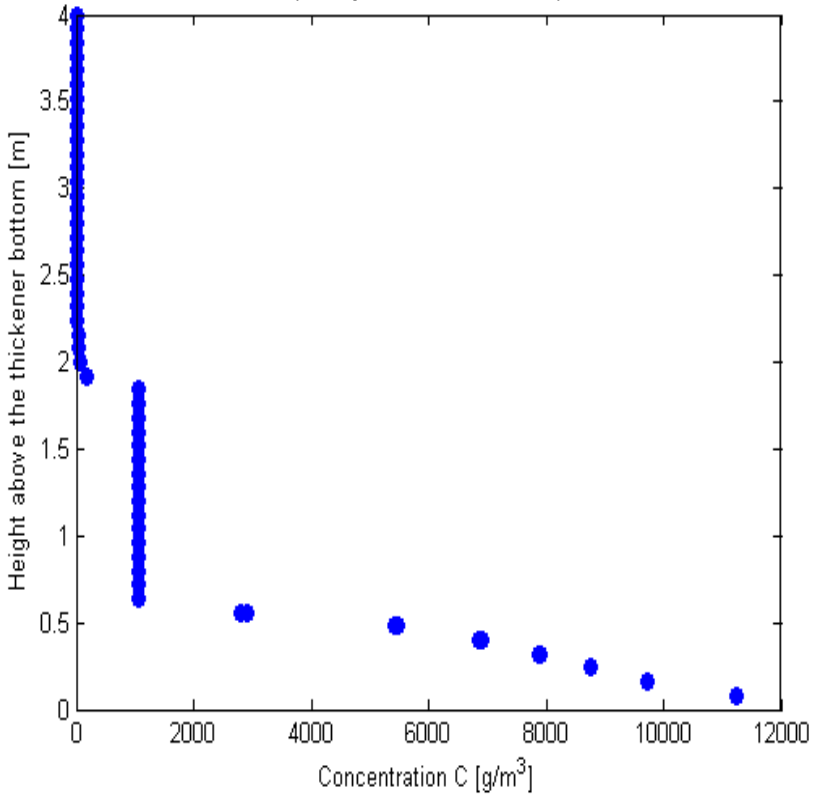

Figure.9- A dynamic solids concentration profile as a function of time and height
(Gravity flux constrain model)

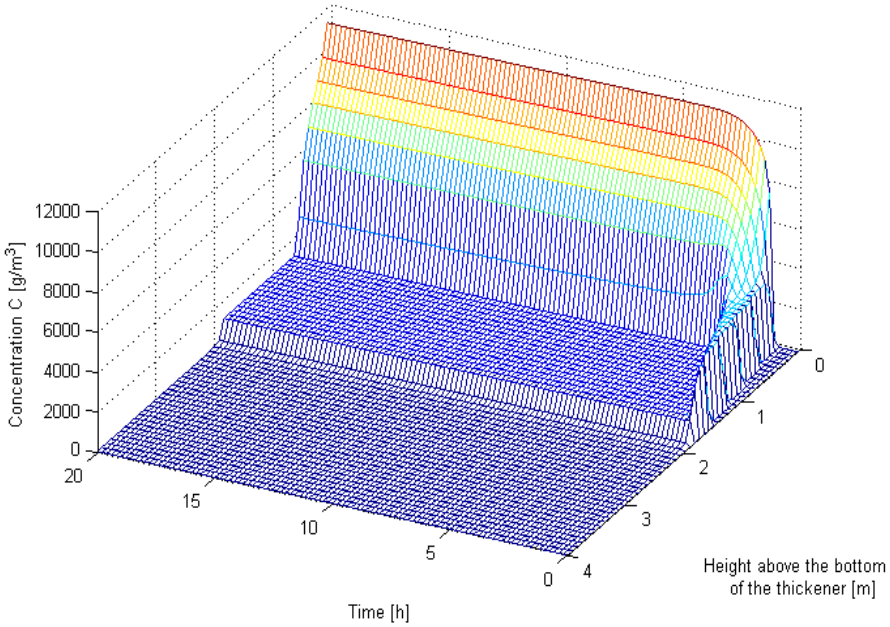

Figure.10-Solids concentration profile
(Dispersion model)

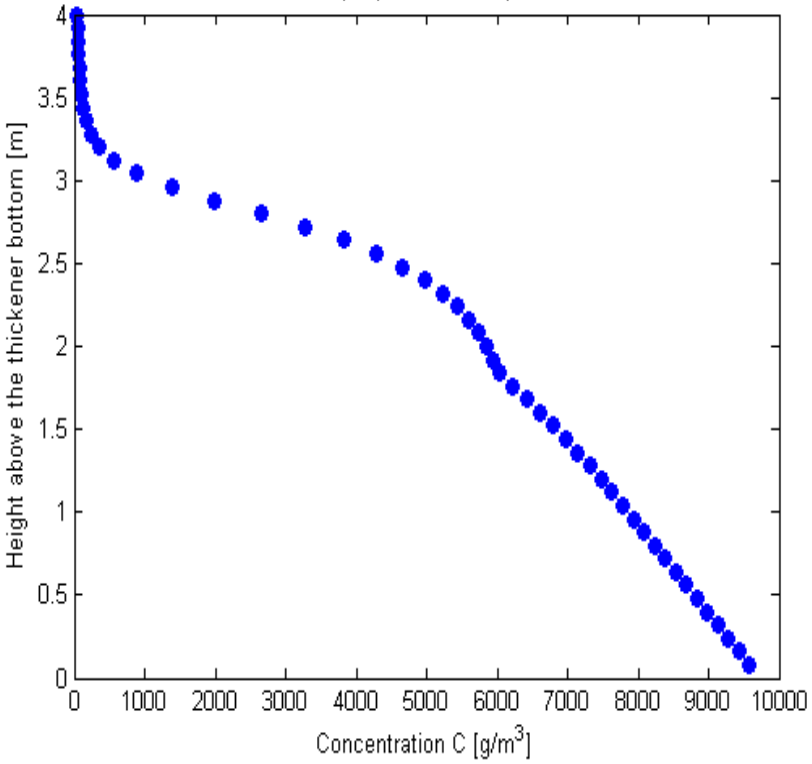

Figure.11- A dynamic solids concentration profile as a function of time and height
(Dispersion model)

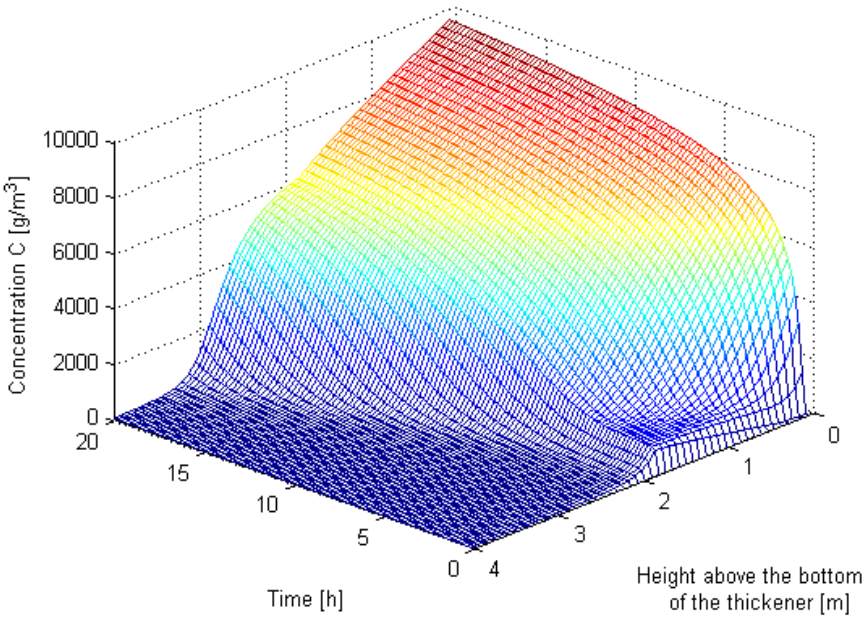

Figure.12-Solids concentration profile
(Gravity flux constrain model)

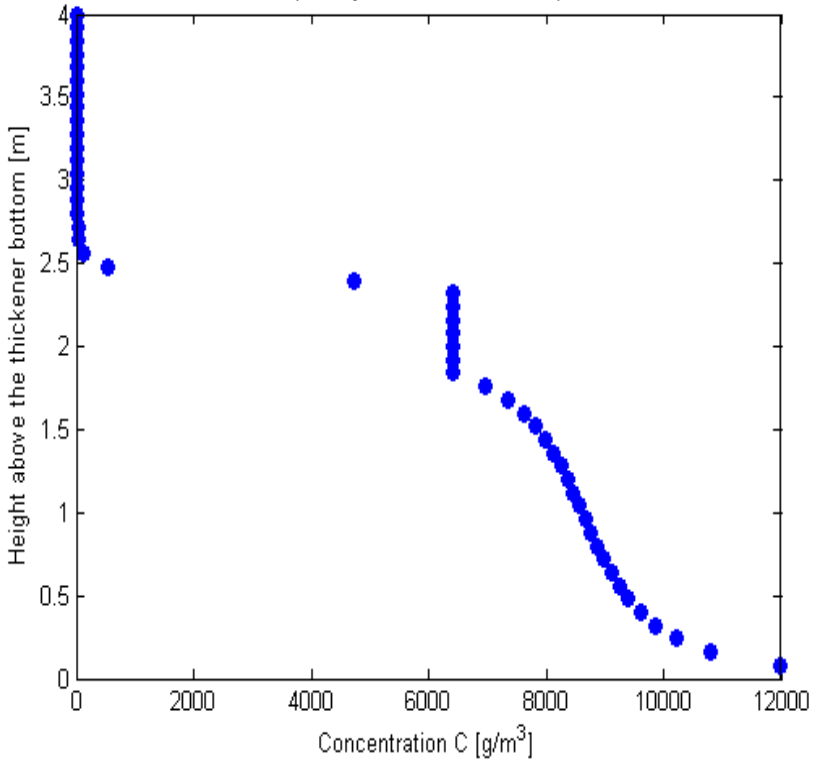

Figure.13- A dynamic solids concentration profile as a function of time and height
(Gravity flux constrain model)

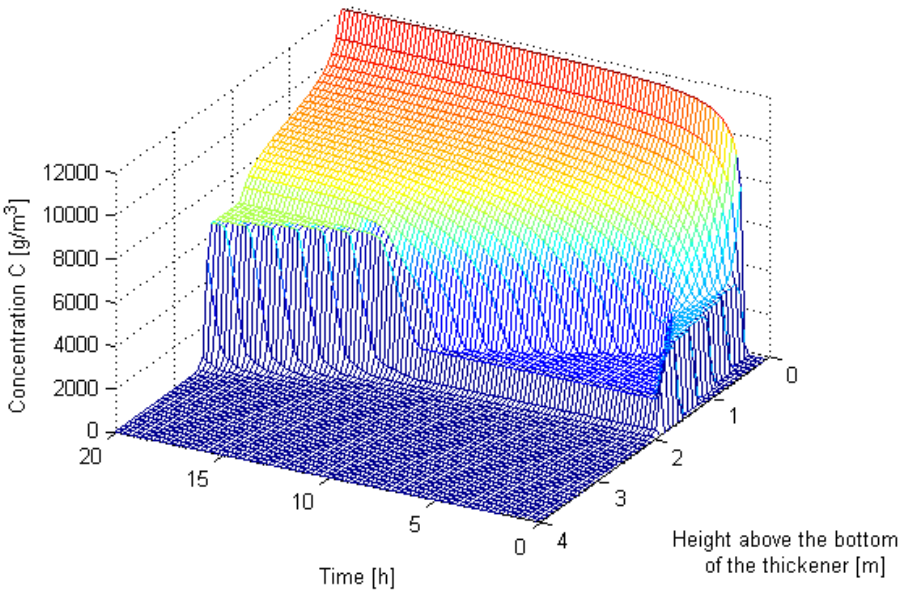

Figure.14-Solids concentration profile
(Dispersion model)

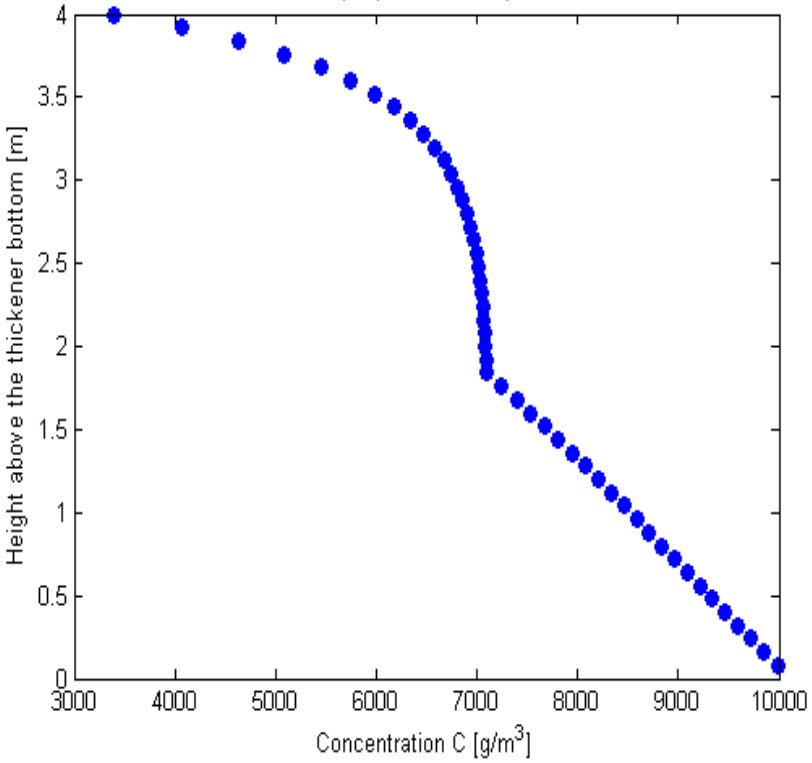

Figure.15- A dynamic solids concentration profile as a function of time and height
(Dispersion model)

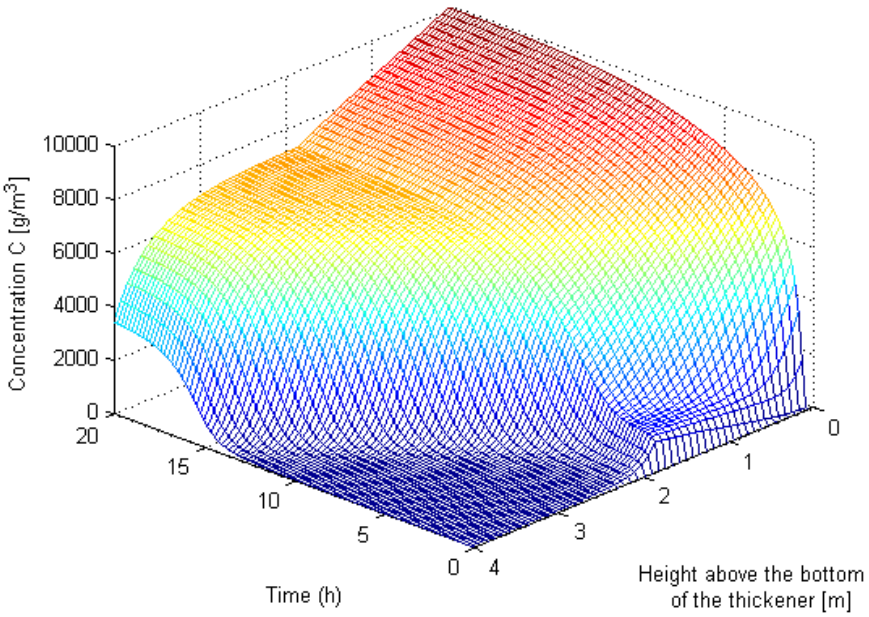

3.3. Flaws of Gravity Flux Constraint Model and Dispersion Model

The gravity flux constraint model and the dispersion model still have flaws in evaluating the continuous settling behavior. One flaw in both of them is sensitivity with respect to the number of layers used in simulation, which means the simulation results are highly dependent on the number of model layers [37, 44, 46]. This is clearly inappropriate, since the solids concentration profiles are totally independent of the number of model layers. Another shortcoming is that these two models can not provide uniform or similar estimations for the same loading situation. The difference in the calculated results between the two models diverge as the number of layers increases.

Table 2- The key variables for Gravity Flux Constraint Model and Dispersion Model in the underloading situation

Variables	Gravity Flux Constraint Model			Dispersion Model		
	10 layers	30 layers	50 layers	10 layers	30 layers	50 layers
$SS_{underflow}$ (g/m^3)	10687	11161	11238	8748.2	9403.2	9578
$SS_{overflow}$ (g/m^3)	18.83	11.55	11.14	42.13	35.71	21.71
Sludge Blanket	2.42	0.92	0.64	2.43	2.61	3.00

Figures 16 to 18 are the static underloading simulation results of 10, 30, 50 layers gravity flux constraint model, and Figures 19 to 21 are the

dynamic results. A particularly interesting observation is the notable difference between the 10-layer result and the 30 and 50 layer results. The effluent solids concentration and the sludge blanket rise rate decrease with an increasing number of layers, while the underflow solids concentration increases and approaches the theoretical value predicted by Hassett method. The changes in solutions for the dispersion model and the gravity flux constraint model with an increasing number of layers in this underloading case are similar.

Several previous investigators have confirmed the sensitivity of the simulation results with the number of layers used in simulation, and shown that increasing the number of layers can profoundly improve the predication accuracy [37, 44, 45]. A minimum of 30-layer has been recommended as the lower limit for gravity flux constraint model and dispersion model simulation [44, 45].

Table 3-The key variables for Gravity Flux Constraint Model and Dispersion Model in the overloading situation

Variables	Gravity Flux Constraint Model			Dispersion Model		
	10 layers	30 layers	50 layers	10 layers	30 layers	50 layers
$SS_{underflow}$ (g/m^3)	11203	11862	11974	9320	9971.6	9986.9
$SS_{overflow}$ (g/m^3)	524.03	22.04	11.18	56.05	3717.7	3393.4
Sludge Blanket	4.00	2.67	2.51	3.27	4.00	4.00

Solids flux theory predicts a continuous slurry blanket height rise starting from the thickener bottom can occur under an overloading condition until the level of the sludge blanket height exceeds the effluent weir. Figures 28 to 39 show the overloading simulation results of gravity flux constraint model and dispersion model with different number of model layers. Although all of these models with different numbers of layers can qualitatively predict the rise of sludge blanket height, the calculated sludge blanket levels at the same time interval are vary greatly. For the gravity flux constraint model, the simulated sludge blanket rise rate decreases with the increase of number of model layer, and the height gradient is 1.49 m between the 10-layer and the 50-layer. However, a larger number of model layers means a more rapid sludge blanket rise according to the dispersion model simulation results, which is contradictory to the gravity flux constraint model's conclusion. Because of a faster sludge blanket raising rate, the 10-layer gravity flux constraint model shows a higher effluent solids concentration, but a lower underflow solids concentration, while the tendencies are contrary in dispersion model with different number of layers.

3.4. Summary of Existing One-Dimensional Clarifier Models

In summary, the essential idea to build a thickener model is division into layers or discretisation. The thickener is divided into several layers along the height, and a continuous equation as equation 37 is built around each

layer based on the mass conservation law. However, as shown previously, the applicability of this original model is quite limited, since it can only give a satisfactory estimation for an underloading clarifier. Two improved approaches are available: Stenstrom's gravity settling flux constraint and Hamilton's dispersion term. Even if they are able to calculate the sludge blanket rise for an overloaded condition, their sensitivity with respect to the number of model layers and the divergence of their predication make the results of limited utility for practical application. Model refinements and advanced numerical methods are needed to improve the simulation quality.

Figure.16-The underloading solids concentration profile of 10 layers
(Graviry flux control model)

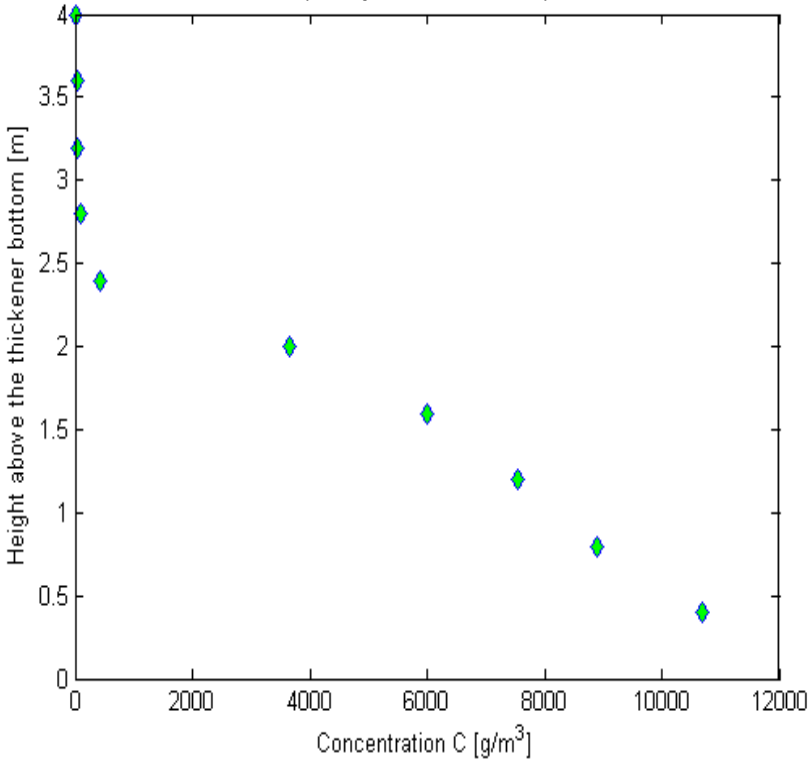

Figure.17-The underloading solids concentration profile of 30 layers
(Graviry flux control model)

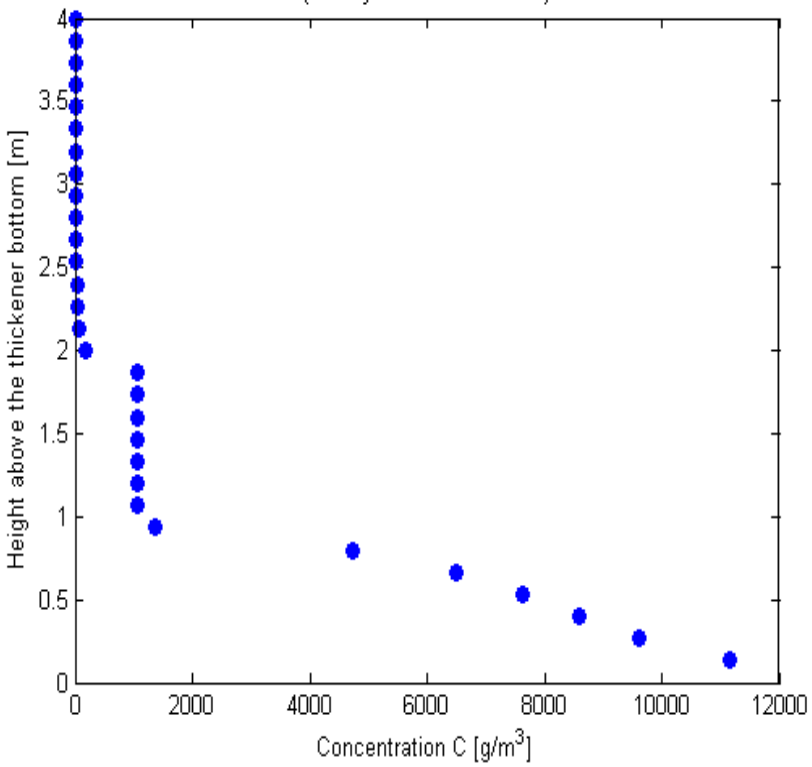

Figure.18-The underloading solids concentration profile of 50 layers
(Graviry flux control model)

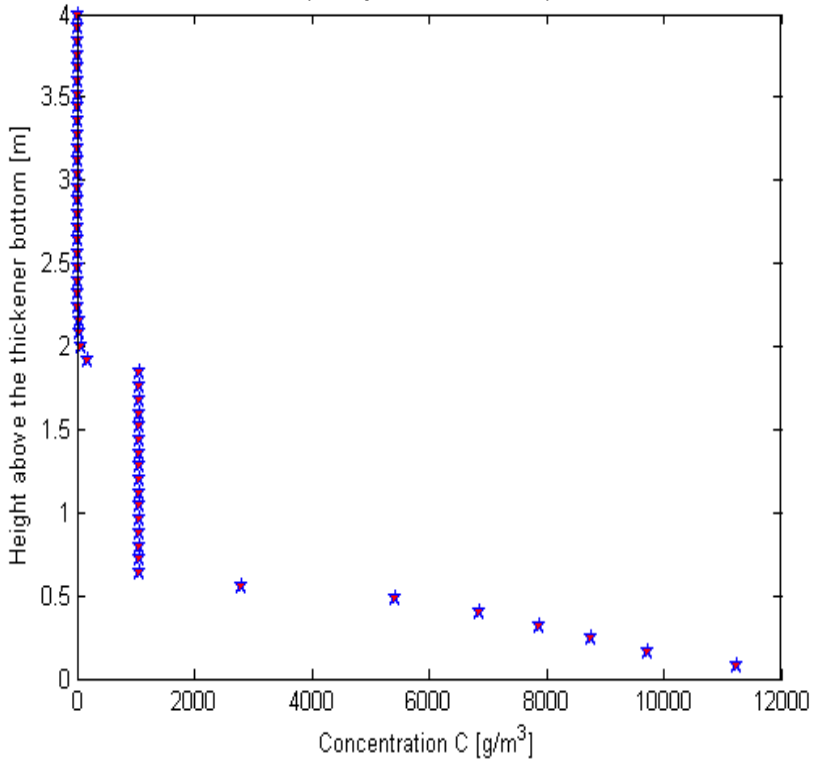

Figure.19- A dynamic underloading solids concentration profile as a function of time and height of 10 layers
(Gravity flux constrain model)

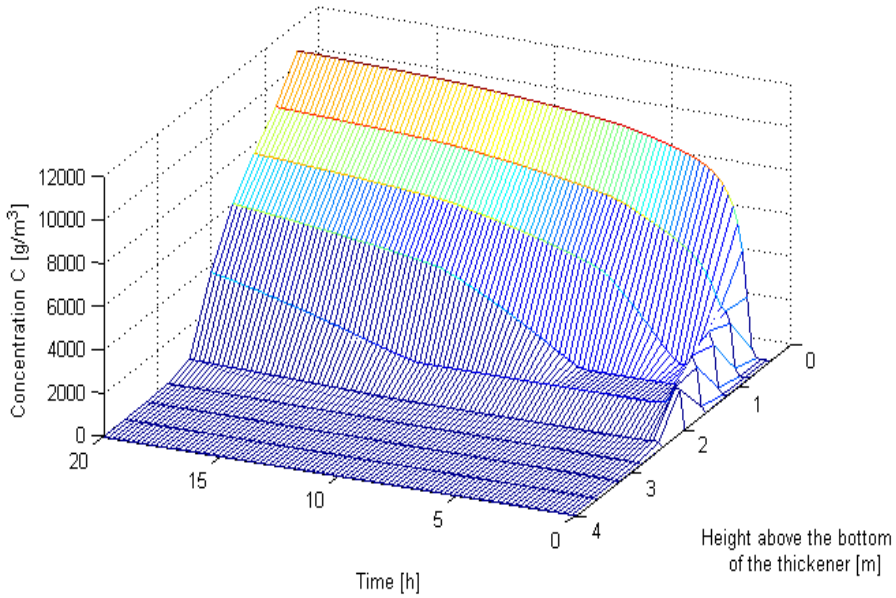

Figure.20- A dynamic underloading solids concentration profile as a function of time and height of 30 layers
(Gravity flux constrain model)

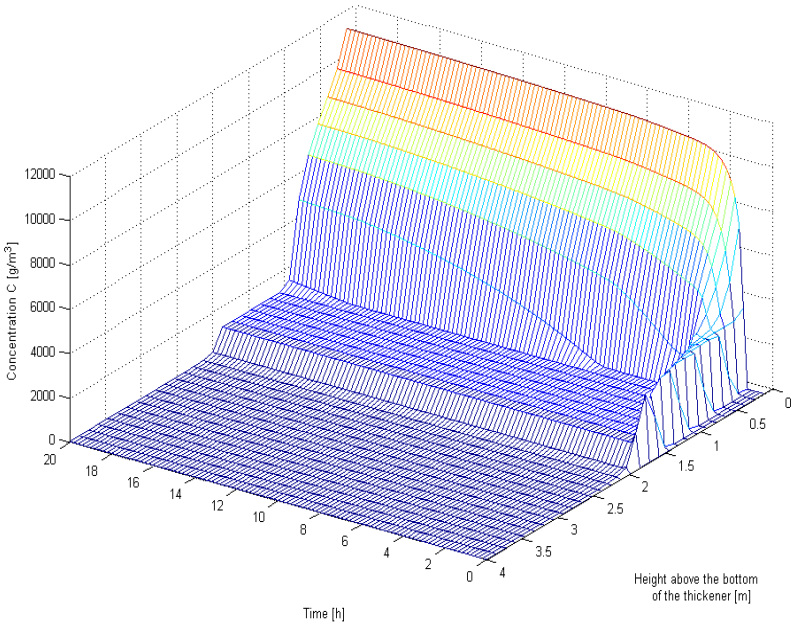

Figure.21- A dynamic underloading solids concentration profile as a function of time and height of 50 layers
(Gravity flux control model)

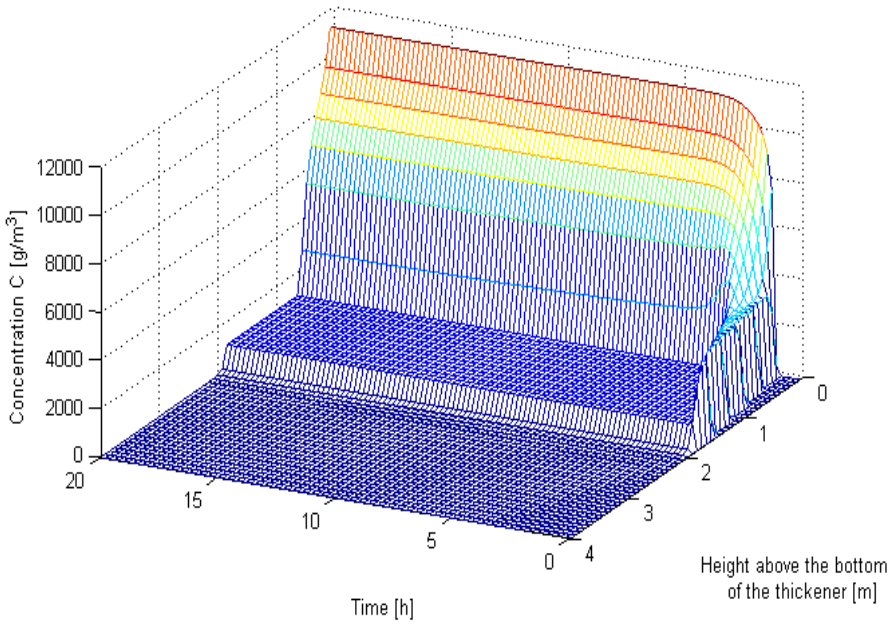

Figure.22-The underloading solids concentration profile of 10 layers
(Dispersion model)

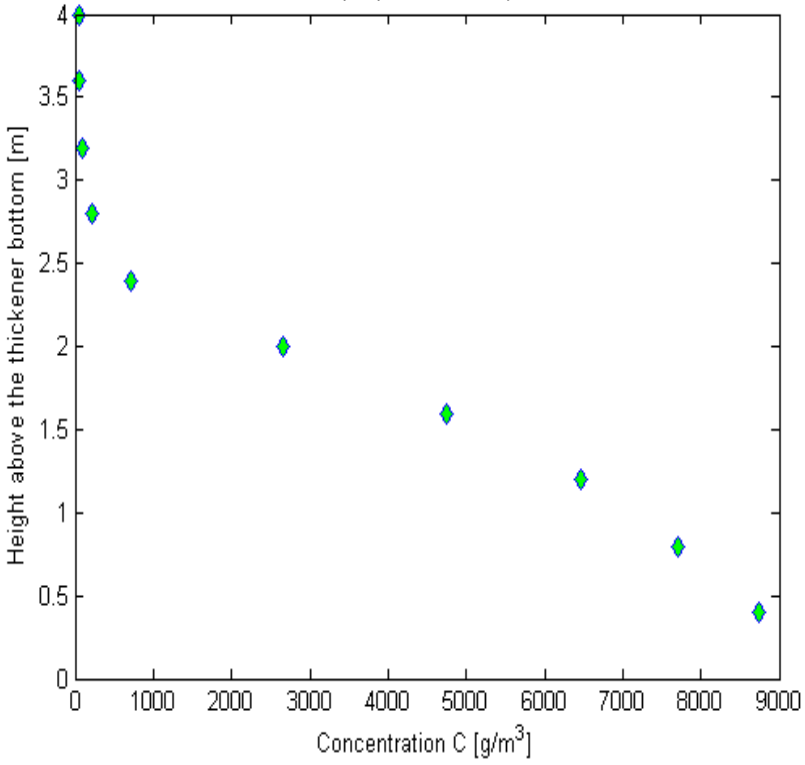

Figure.23-The underloading solids concentration profile of 30 layers
(Dispersion model)

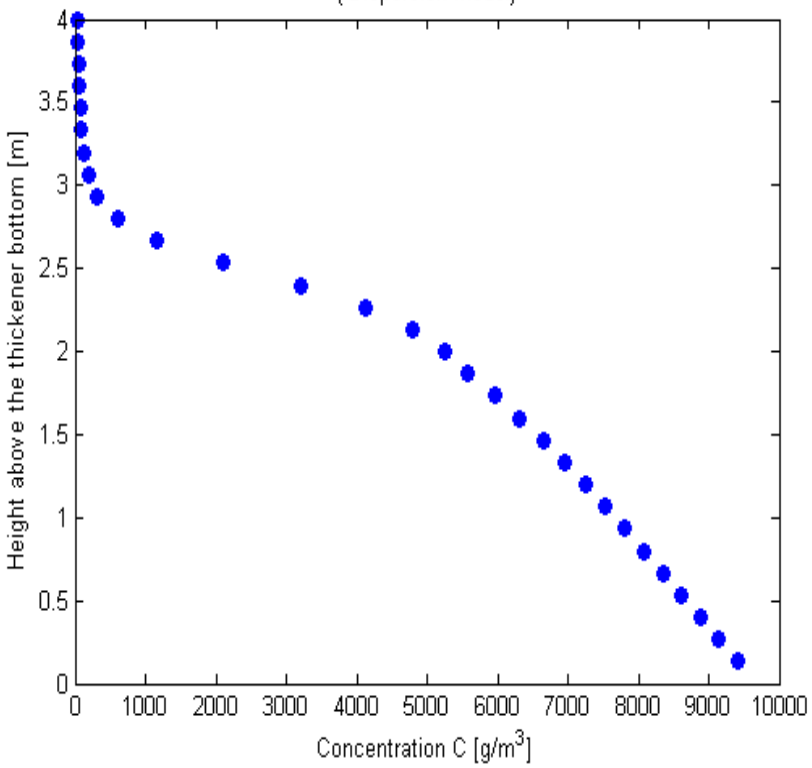

Figure.24-The underloading soldis concentration profile of 50 layers
(Dispersion model)

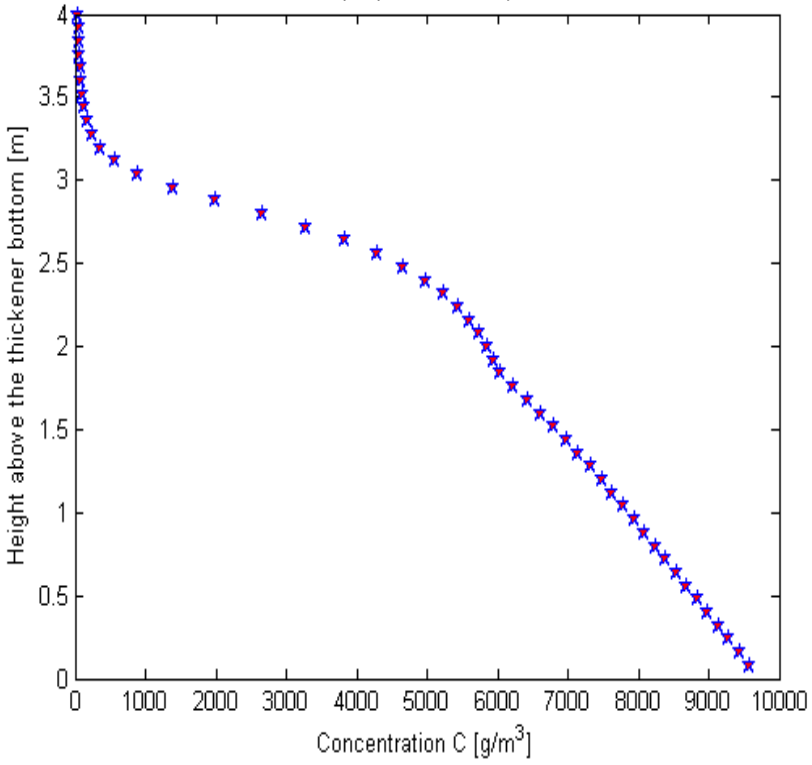

Figure.25-A dynamic underloading solids concentration profile as a function of time and height of 10 layers
(Dispersion model)

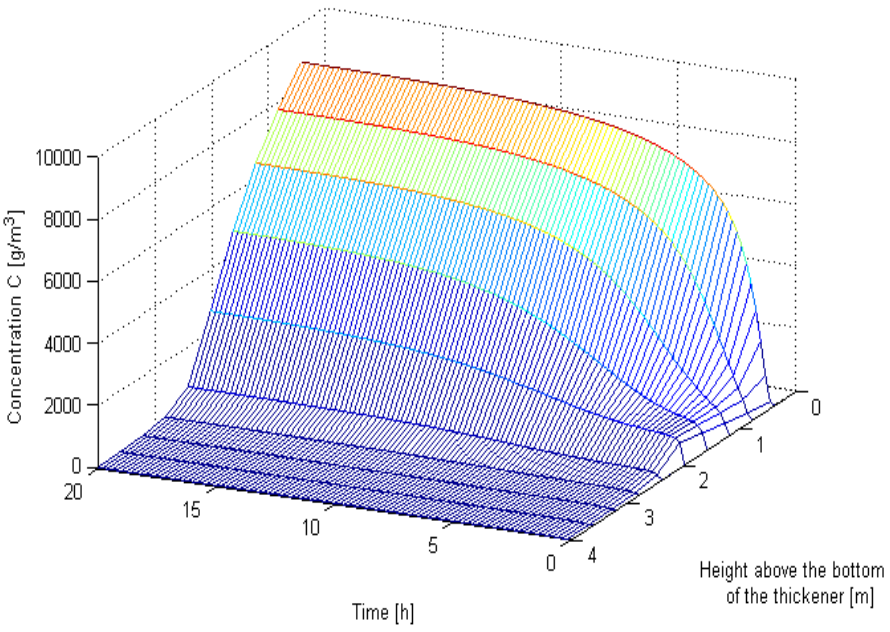

Figure.26-A dynamic underloading solids concentration profile as a function of time and height of 30 layers (Dispersion model)

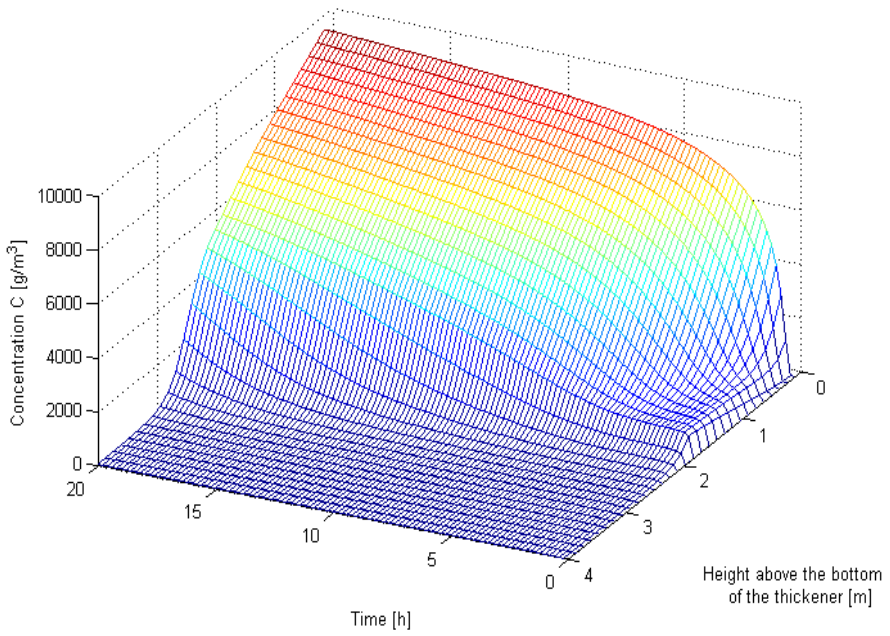

Figure.27-A dynamic underloading solids concentration profile as a function of time and height of 50 layers (Dispersion model)

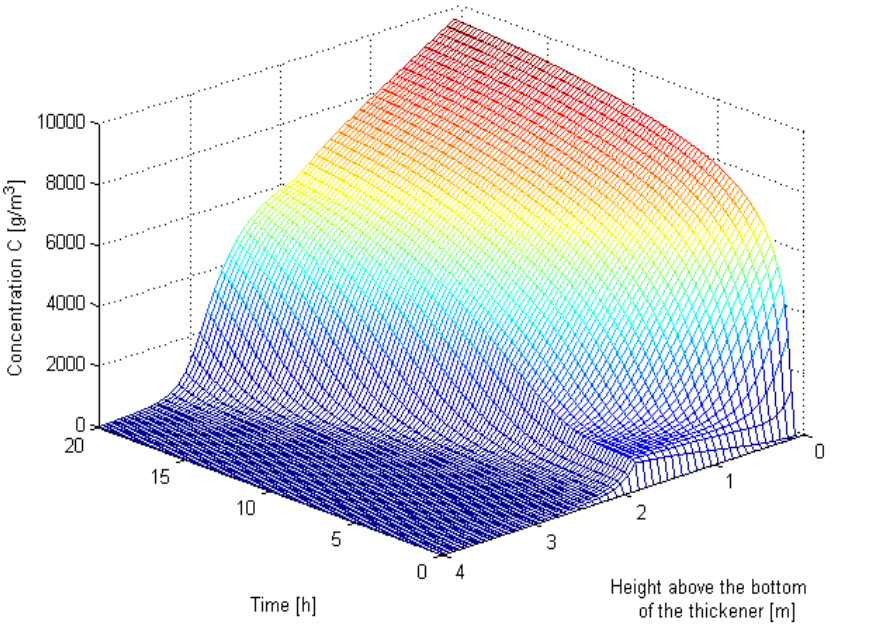

Figure.28-The overloading solids concentration profile of 10 layers
(Gravity flux constrain model)

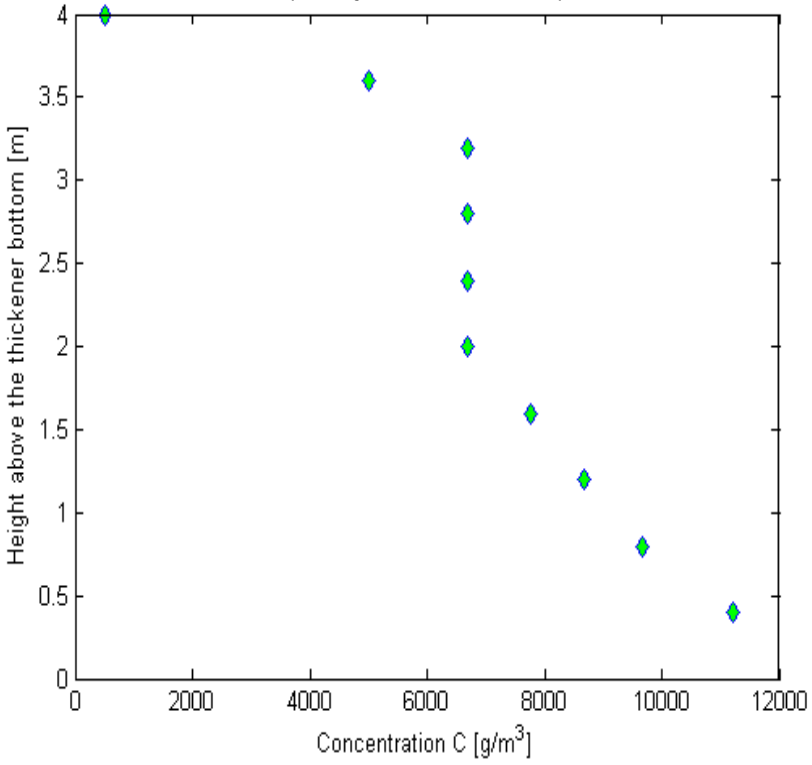

Figure.29-The overloading solids concentration profile of 30 layers
(Graviry flux control model)

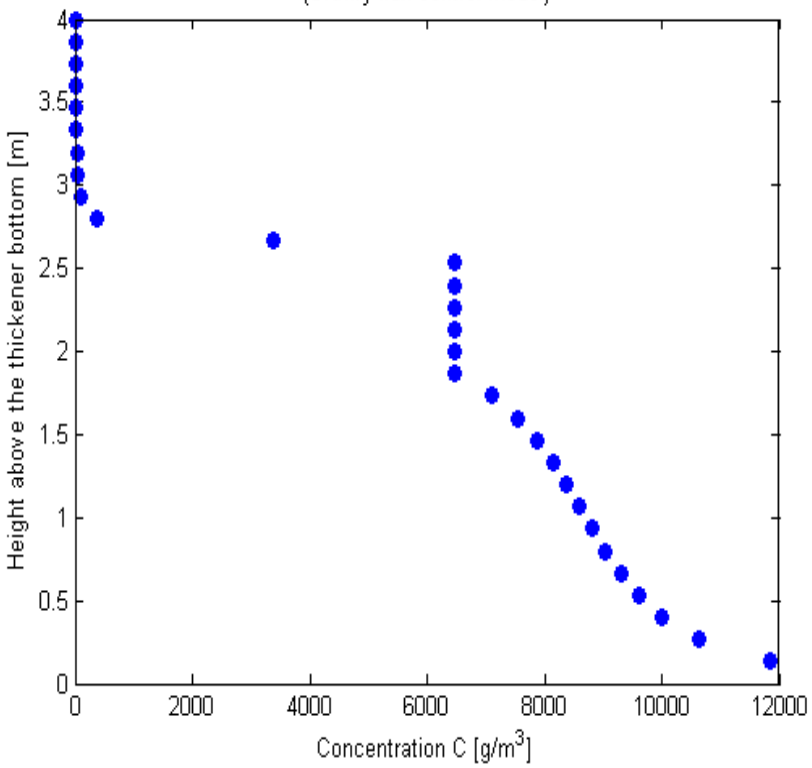

Figure.30-The overloading solids concentration profile of 50 layers
(Graviry flux control model)

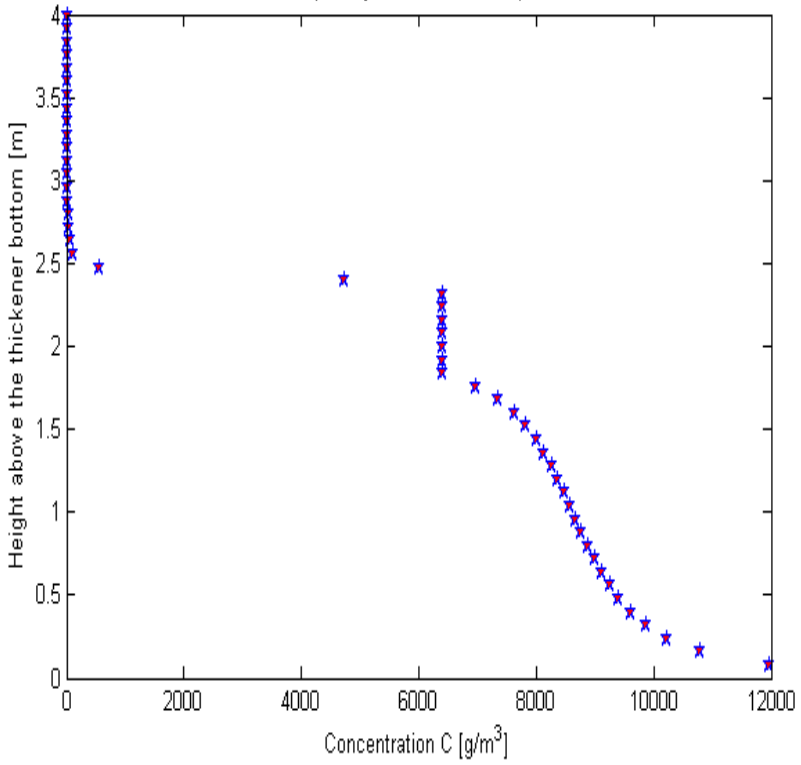

Figure.31-The overloading solids concentration profile of 10 layers
(Dispersion model)

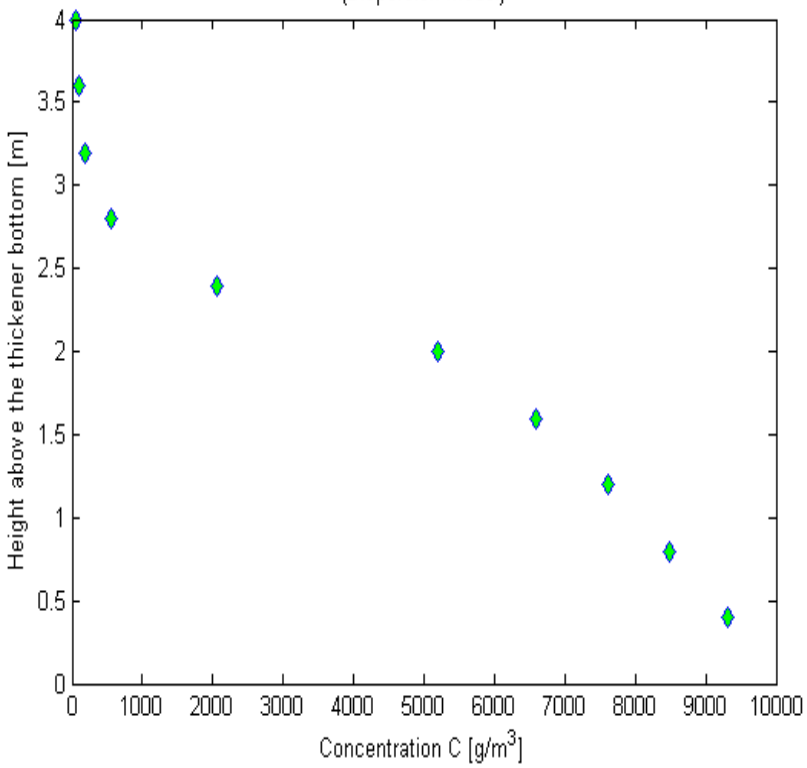

Figure.32-The overloading solids concentration profile of 30 layers
(Dispersion model)

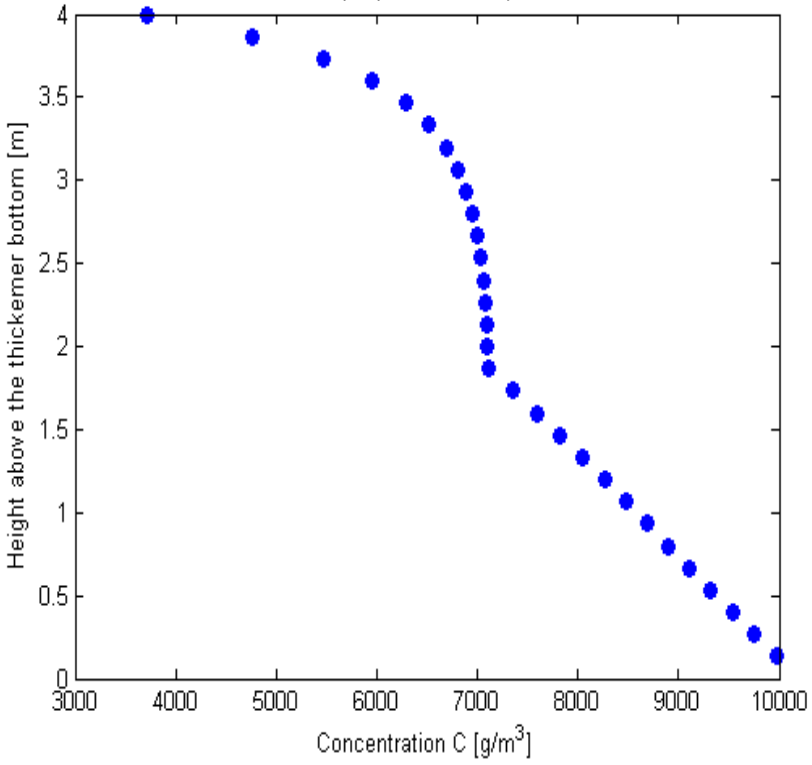

Figure.33-The overloading solids concentration profile of 50 layers
(Dispersion model)

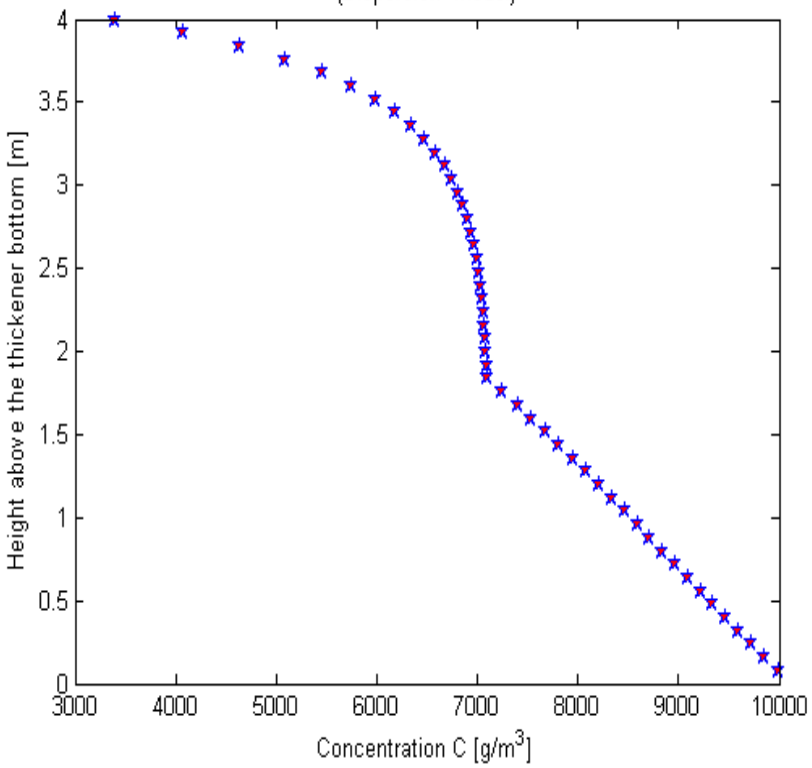

Figure.35- A dynamic overloading solids concentration profile as a function of time and height of 30 layers
(Gravity flux constrain model)

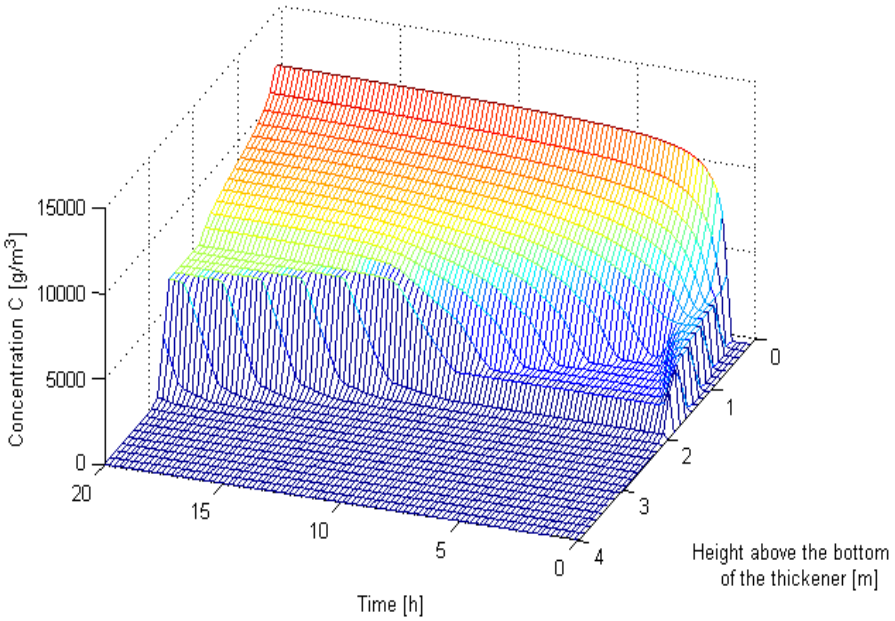

Figure.34- A dynamic overloading solids concentration profile as a function of time and height of 10 layers
(Gravity flux constrain model)

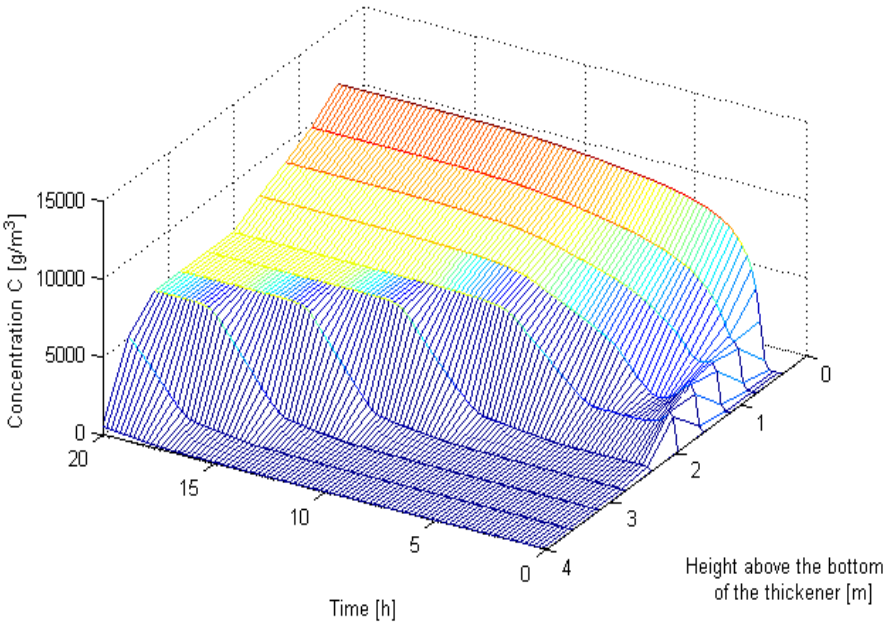

Figure.36- A dynamic overloading solids concentration profile as a function of time and height of 50 layers
(Gravity flux constrain model)

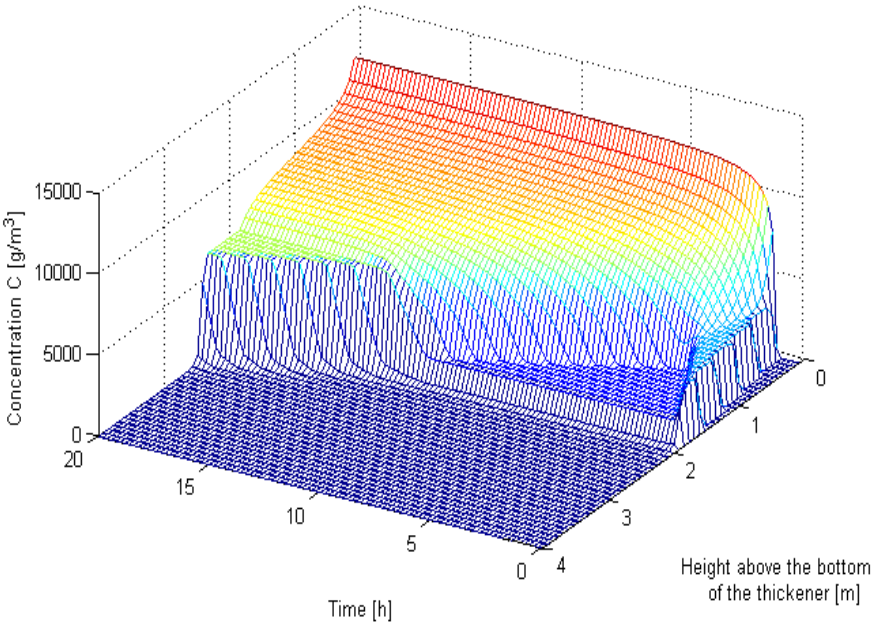

Figure.37- A dynamic overloading solids concentration profile as a function of time and height of 10 layers
(Gravity flux constrain model)

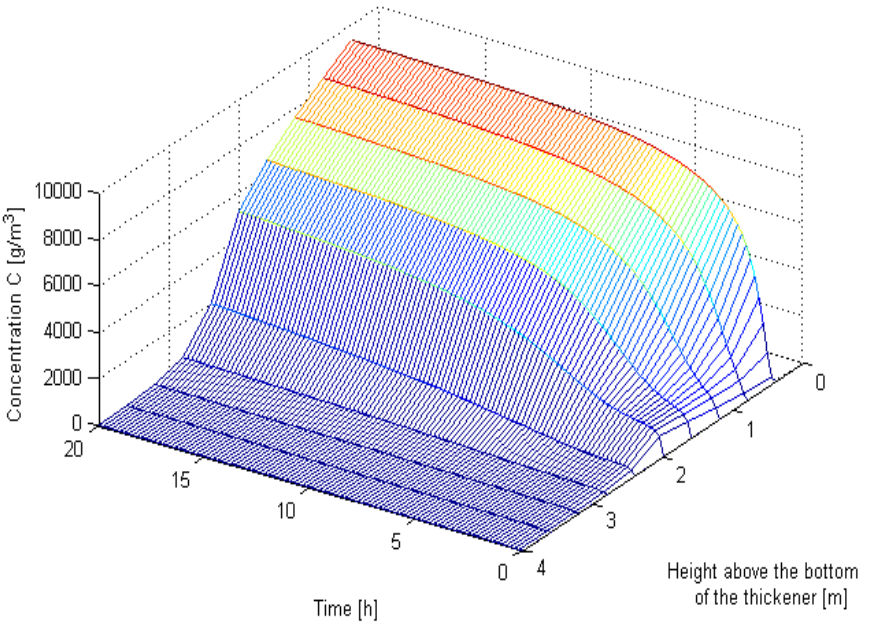

Figure.38- A dynamic overloading solids concentration profile as a function of time and height of 30 layers (Dispersion model)

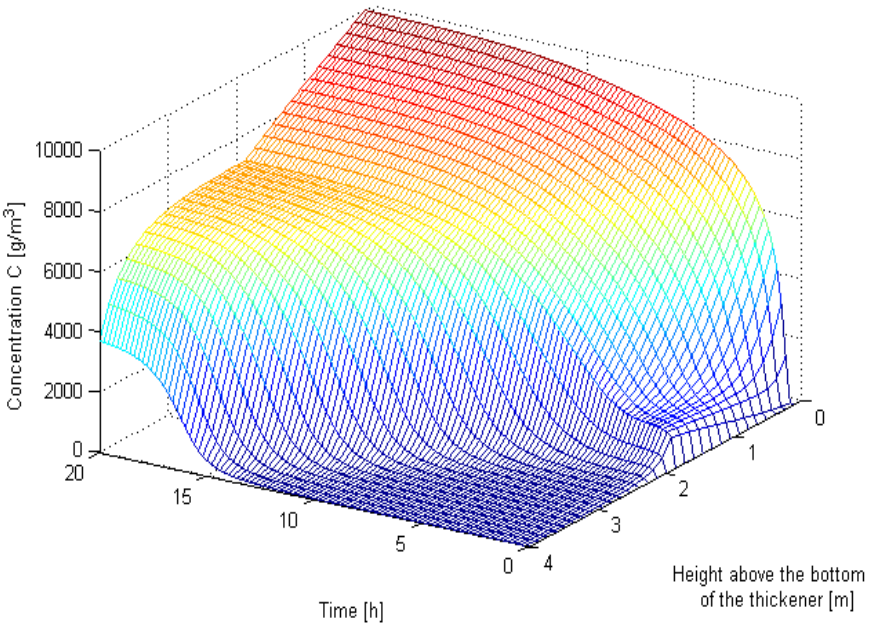

Figure.39-A dynamic overloading solids concentration profile as a function of time and height of 50 layers (Dispersion model)

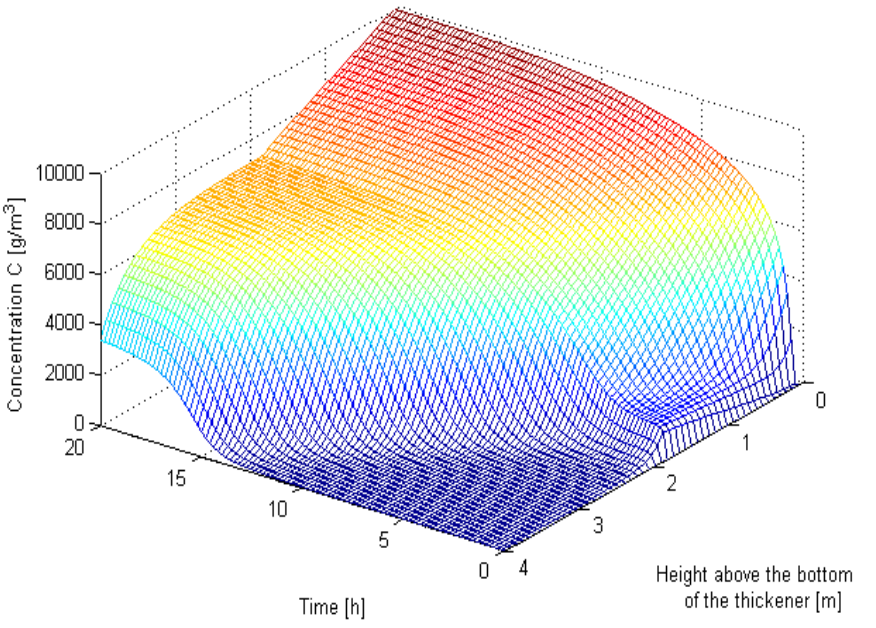

3.5. Method of Characteristics

The Method of characteristic (MOC) is a mathematic technique for solving partial differential equations. Typically, MOC is used to solve the initial value problem for first-order hyperbolic partial differential equations. The essential strategy of this numerical method is to reduce a partial differential equation to a collection of ordinary equations. Application of MOC to solve hyperbolic partial differential equations, especially for quasilinear and nonlinear problems, is highly dependent on identifying the characteristic curve or characteristic line. Only along the characteristic line can a solution be integrated from the given initial values.

Equation 52-61 is a simple example to show how the MOC can be used to solve a quasilinear first-order hyperbolic partial differential equation.

$$\begin{cases} \dfrac{\partial u}{\partial t} + (x+t)\dfrac{\partial u}{\partial t} + u = x & x \in R, t > 0 \quad (52) \\ u(x,0) = x & x \in R \quad (53) \end{cases}$$

Step one: calculate the characteristic line

$$\begin{cases} \dfrac{\partial x}{\partial t} = x + t & t > 0 \quad (54) \\ x(0) = c \quad (55) \end{cases}$$

Characteristic line: $x(t) = (1+c)e^{t} - (t+1)$

Step two: set $U(t) = u(x(t), t)$

$$\begin{cases} \dfrac{dU(t)}{dt} + U(t) = (1+c)e^{t} - (t+1) & t > 0 \quad (56) \\ U(0) = u(x(0),0) = u(c,0) = c \quad (57) \end{cases}$$

$$U(t) = \frac{1}{2}(c+1)e^{t} + \frac{1}{2}(c-1)e^{-t} - t \quad (58)$$

Step three: $u(x(t),t) = U(t) = \frac{1}{2}(c+1)e^{t} + \frac{1}{2}(c-1)e^{-t} - t$

$$x(t) = (1+c)e^{t} - (t+1) \Rightarrow c = [x(t) + t + 1]e^{-t} - 1 \quad (59)$$

$$u(x(t),t) = \frac{1}{2}[x(t) + t + 1]e^{-2t} - e^{-t} + \frac{1}{2}[x(t) - t + 1] \quad (60)$$

$$u(x,t) = \frac{1}{2}(x + t + 1)e^{-2t} - e^{-t} + \frac{1}{2}(x - t + 1) \quad (61)$$

3.6. Possibility and Difficulty of Using Method of Characteristics

An important, frequently used partial differential equation is for the conservation of mass, momentum or energy. The original dynamic model, equation 37, was based on mass conservation around each layer and can be expressed as follows:

$$\frac{\partial C(z,t)}{\partial t} + \frac{\partial G_s(C(z,t))}{\partial z} + u\frac{\partial C(z,t)}{\partial z} = s(t)\delta(z) \quad (37)$$

It is noteworthy that this partial differential equation is a nonlinear first-order partial differential equation. Therefore the MOC can be used to

solve this equation with the obvious advantage that the essential strategy of MOC is convert a partial differential equation to a collection of ordinary differential equations, and integrate the solution along the characteristic lines, instead of replacing the partial derivatives by their finite-difference approximations and calculating the solution layer by layer. Consequently, the solution presented by MOC can be totally independent of the number of model layers and overcome the problem caused by discretisation.

Based on the assumption that the gravity settling velocity is only determined by the local solids concentration, equation 35 in thickening and clarification zone can also be expressed as follows:

$$\frac{\partial C(z,t)}{\partial t} + v(c)\frac{\partial C(z,t)}{\partial z} + u\frac{\partial C(z,t)}{\partial z} = 0 \tag{62}$$

$$\begin{cases} \dfrac{\partial C(z,t)}{\partial t} + \left(v(c)+u\right)\dfrac{\partial C(z,t)}{\partial z} = 0 & (63) \\ dC = dt\dfrac{\partial C}{\partial t} + dz\dfrac{\partial C}{\partial z} & (64) \end{cases}$$

The equation set can be expressed in the following matrix

$$\begin{bmatrix} 1 & v(c)+u \\ dt & dz \end{bmatrix} \begin{bmatrix} \dfrac{\partial C}{\partial t} \\ \dfrac{\partial C}{\partial z} \end{bmatrix} = \begin{bmatrix} 0 \\ dC \end{bmatrix} \tag{65}$$

To calculate the characteristic line, set the determinate equal to zero and

solve for the roots, as follows:

$$\begin{bmatrix} 1 & v(c)+u \\ dt & dz \end{bmatrix} = 0 \Rightarrow \frac{dz}{dt} = v(c)+u \tag{66}$$

There the characteristic line is:

$$\frac{dz}{dt} = v(c)+u \tag{67}$$

Figure 40-The sketch profile of the characteristic line

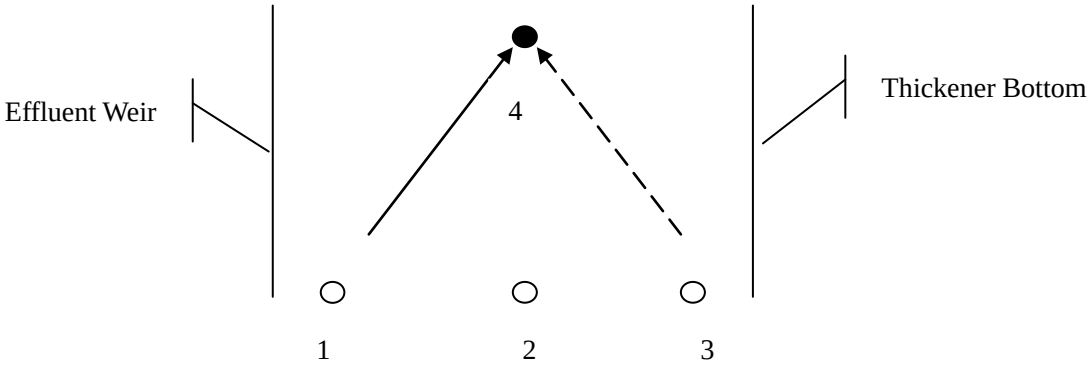

According to Figure 40, the characteristic line (the solid line) calculated in equation 48 is always a positive characteristic line, meaning its direction is from the feed point or effluent weir to the thickener bottom. So the value of the black grid 4 is affected by the point 1, since the information propagates along the positive characteristic line. From physical observations, the value of point 4 is also affected by the downstream point, such as point 3, especially under an overloading condition, when the sludge blanket level rises from the thickener bottom.

The downstream information can propagate along a negative characteristic line (the dotted line). However, Figure 40 shows that the mass conservation equation 45 can not provide such a negative characteristic line, so the single mass conservation partial differential equation is not a sufficient condition for using MOC to calculate the routinely observed concentration profile during clarifier overloading. Another partial differential equation is necessary to provide the negative characteristic line, and such partial differential equation can be formed based on the momentum, energy conservation law. Further investigations need to be conducted to develop the solution. .

4. CONCLUSION

1. In order to reduce the computational burden, biological models are mostly combined with the 1-D secondary clarifier model to simulate the biological waster water treatment by the activated sludge process. By dividing the clarifier into several layers, a partial differential equation can be formed based on the mass conservation law around each layer, and this original model has been demonstrated to be effective in predicting the effluent and underflow solids concentration for underloading conditions. For overloaded conditions, the model fails to predict the routinely observed clarifier failures. It fails to predict the rise of sludge blanket level, and the calculated underflow solids concentration also exceeds the observed maximum value. In conclusion, the original model is able to predict only under loaded conditions, which is unfortunate, since overloaded conditions are the conditions of interest. Under loaded conditions are of less interest because under loaded clarifiers do not fail from rising sludge blankets.

2. Two different strategies are available as improvements of the original model: adding a constraint to limit the gravity flux or adding a dispersion term to convert the initial first-order hyperbolic partial differential equation to a secondary-order parabolic partial differential equation. The simulation results confirm the fact that both of them can predict the sludge blanket height rise in an overloading condition.

However, comparable simulations running the two improved models with same parameters show that the two models' simulation results differ from each other, and the dispersion model even fails in predicating the underloading settling behavior. In addition to the differences in simulation results between two models, both models are sensitive to the number of model layers, which means the simulation results are highly dependent on the number of layers. Some previous investigators suggested that at least 30-layers model are necessary to guarantee high estimation quality. An interesting observation is that the change tendencies of the predicted effluent solids concentration and the sludge blanket rise rate of two models are opposite; as a result, the increasing of model layers can not improve the performance of the gravity flux constraint model and the dispersion model simultaneously.

3. Method of characteristic (MOC) is a mathematic technique to solve partial differential equations, and is especially effective in solving first-order hyperbolic equations. Given the fact that the original model equation is a nonlinear partial differential equation, MOC can be used to solve it without introducing the layers sensitive problem, since the main idea of MOC is convert the partial differential equation to series of ordinary differential equations and then integrate along the characteristic line. A brief analysis indicates that the single mass conservation equation can provide only a positive characteristic line (downward sloped), an upper layer cannot be impacted by a lower layer, which is the opposite of physical observations. A second partial

differential equation is required to calculate a negative or upward pointing characteristic line, and this equation should be built upon the momentum or energy conservation.

REFERENCE LIST

1. Alderton JL: **Discussion of " Analysis of Thickerer Operation." by V. C.Behn and J. C. Liebman**. *Jour San Eng Div ASCE* 1963, **89**(6):57-59.

2. Takacs I, Patry GG, Nolasco D: **A Dynamic-Model of the Clarification Thickening Process**. *Water Res* 1991, **25**(10):1263-1271.

3. Tracy KD: **Mathematical Modeling of Unsteady-State Thickening of Compressible Slurries**. *PhD Dissertation* 1973, **Clemson University. Clemson, South Carolina**.

4. Coe HB, Clevenger GH: **Methods for determining the capacities of slime-settling tanks**. *T Am I Min Met Eng* 1916, **55**:356-384.

5. Comings EW, Pruiss CE, Debord C: **CONTINUOUS SETTLING AND THICKENING**. *Industrial and Engineering Chemistry* 1954, **46**(6):1164-1172.

6. Kynch GJ: **A Theory of Sedimentation**. *T Faraday Soc* 1952, **48**(2):166-176.

7. Kynch GJ: **A Note on Exchange Magnetic Moments**. *Phys Rev* 1951, **81**(6):1060-1061.

8. Talmage WP, Fitch EB: **Determining Thickener Unit Areas**. *Industrial and Engineering Chemistry* 1955, **47**(1):38-41.

9. Behn VC: **Settling Behavior of Waste Suspensions**. *Jour San Eng Div ASCE* 1957, **83**(5):20.

10. Roberts EJ: **Thickening - Art or Science**. *T Am I Min Met Eng* 1949, **184**(3):61-64.

11. Eckenfelder WW, Melbinger N: **Settling and Compaction Characteristics of Biological Sludges .1. General Considerations**. *Sewage Ind Wastes* 1957, **29**(10):1114-1122.

12. Hassett NJ: **Design and Operation of Continuous Thickeners**. *Industrial Chemist* 1958, **34**:116-120.

13. Fitch B: **Sedimentation Process Fundamentals**. *T Soc Min Eng* 1962, **223**(2):129-137.

14. Moncrieff AG: **Theory of Thickener Design Based on Batch Sedimentation Tests**. *Trans Inst Min and Met* 1964, **73**:729-761.

15. Scott KJ: **Thickening of Calcium Carbonate Slurries - Comparison of Data with Results for Rigid Spheres**. *Ind Eng Chem Fund* 1968, **7**(3):484-&.

16. Scott KJ: **Experimental Study of Continuous Thickening of a Flocculated Silica Slurry**. *Ind Eng Chem Fund* 1968, **7**(4):582-&.

17. Scott KJ: **Continuous Thickening of Flocculated Suspensions - Comparison with Batch Settling Tests and Effects of Floc Compression Using Pyrophyllite Pulp**. *Ind Eng Chem Fund* 1970, **9**(3):422-&.

18. Dick RI: **Applicability of Prevailing Thickening Theories to Activated Sludge.** *PhD Dissertation* 1965, **University of Illinois. Urbana, Illinois**.

19. Kammermeyer K: **Settling and thickening of aqueous suspensions**. *Industrial and Engineering Chemistry* 1941, **33**:1484-1491.

20. Behn VC: **Settling Behavior of Waste Suspensions**. *Jour San Eng Div ASCE* 1957, **83**(5):1-20.

21. Work LT, Kohler AS: **The sedimentation of suspensions**. *T Am Inst Chem Eng* 1940, **36**(5):0701-0719.

22. Shannon PT, Stroupe E, Tory EM: **Batch and Continuous Thickening - Basic Theory - Solids Flux for Rigid Spheres**. *Ind Eng Chem Fund* 1963, **2**(3):203-&.

23. Shannon PT, Tory EM: **Settling of Slurries - New Light on an Old Operation**. *Industrial and Engineering Chemistry* 1965, **57**(2):18-&.

24. Comings EW: **Thickening of Calcium Carbonate Slurries.** *Ind Eng Chem Fund* 1940, **32**:663-667.

25. Yoshioka N, Y. Hotta, S. Tanaka, S. Naito, S. Tsugami. : **Continuous Thickening of Homogeneous Flocculated Suspensions.** *Kagaku Kogaku* 1957, **21**:66-74.

26. Hassett NJ: **Concentrations in a Continuous Thickener.** *Industrial Chemist* 1964, **40**:29-33.

27. Tory EM, Shannon PT: **Subsicence of Slimes**. *J Colloid Interf Sci* 1966, **21**(1):107-&.

28. Tory EM, Shannon PT: **Reappraisal of Concept of Settling in Compression - Settling Behavior and Concentration Profiles for Initially Concentrated Calcium Carbonate Slurries**. *Ind Eng Chem Fund* 1965, **4**(2):194-&.

29. Dick RIaARJ: **Continuous Thickening of Non-Ideal Suspensions**. *WRC Research Report No 45* 1972, **University of Illinois**:Urbana, Illinois.

30. Javaheri AB: **Continuous Thickening of Non-Ideal Suspensions.** *PhD Dissertation* 1971:University of Illinois. Urbana, Illinois. 1971. .

31. Edde HJWWE: **Theoretical Concepts of Gravity Sludge Thickening and Methods of Scale-up from Laboratory Units to Prototype Design**. *CRWR-15* 1967:University of Texas. Austin, Texas.

32. Bryant J: **Continuous Time Simulation of the Conventional Activated Sludge Wastewater Renovation System.** *PhD Dissertation* 1972:Clemson University. Clemson, South Carolina.

33. Stenstrom MK: **A dynamic model and computer compatible control strategies for wastewater treatment plants.** *PhD Dissertation* 1976:Clemson University. Clemson, South Carolina.

34. Vitasovic ZZ: **An Integrated Control Strategy for The Activated Sludge Process.** *PhD Dissertation* 1986: Rice University, Houston, Tex. .

35. Laikari H: **Simulation of the Sludge Blanket of a Vertical Clarifier in an Activated-Sludge Process**. *Water Sci Technol* 1989, **21**(6-7):621-629.

36. Vesilind PA: **Discussion of "Evaluation of Activated Sludge Thickening Theories" By R. I. Dick and B. B. Ewing**. *Jour San Eng Div ASCE* 1968, **94**:185-191.

37. Hamilton J, Jain R, Antoniou P, Svoronos SA, Koopman B, Lyberatos G: **Modeling and Pilot-Scale Experimental-Verification for Predenitrification Process**. *J Environ Eng-Asce* 1992, **118**(1):38-55.

38. Hartel L, Popel HJ: **A Dynamic Secondary Clarifier Model Including Processes of Sludge Thickening**. *Water Sci Technol* 1992, **25**(6):267-284.

39. Otterpohl R, Freund M: **Dynamic-Models for Clarifiers of Activated-Sludge Plants with Dry and Wet Weather Flows**. *Water Sci Technol* 1992, **26**(5-6):1391-1400.

40. Dupont R, Henze M: **Modeling of the Secondary Clarifier Combined with the Activated-Sludge Model No 1**. *Water Sci Technol* 1992, **25**(6):285-300.

41. Grijspeerdt K, Vanrolleghem P, Verstraete W: **Selection of One-Dimensional Sedimentation - Models for Online Use**. *Water Sci Technol* 1995, **31**(2):193-204.

42. Dupont R, Dahl C: **A One-Dimensional Model for a Secondary Settling-Tank Including Density-Current and Short-Circuiting**. *Water Sci Technol* 1995, **31**(2):215-224.

43. Plosz BG, Weiss M, Printemps C, Essemiani K, Meinhold J: **One-dimensional modelling of the secondary clarifier-factors affecting simulation in the clarification zone and the assessment of the thickening flow dependence**. *Water Res* 2007, **41**(15):3359-3371.

44. Jeppsson U, Diehl S: **An evaluation of a dynamic model of the secondary clarifier**. *Water Sci Technol* 1996, **34**(5-6):19-26.

45. David R, Saucez P, Vasel JL, Wouwer AV: **Modeling and numerical simulation of secondary settlers: A Method of Lines strategy**. *Water Res* 2009, **43**(2):319-330.

46. Watts RW, Svoronos SA, Koopman B: **One-dimensional modeling of secondary clarifiers using a concentration and feed velocity-dependent dispersion coefficient**. *Water Res* 1996, **30**(9):2112-2124.

47. De Clercq J, Devisscher M, Boonen I, Vanrolleghem PA, Defrancq J: **A new one-dimensional clarifier model - verification using full-scale experimental data**. *Water Sci Technol* 2003, **47**(12):105-112.

48. Clercq J: **Batch and Continuous Settling of Activated Sludge: In-Depth Monitoring and 1D Compression Modelling.** *PhD Dissertation* 2007:Department of Chemical Engineering, Ghent University,.

49. De Clercq J, Nopens I, Defrancq J, Vanrolleghem PA: **Extending and calibrating a mechanistic hindered and compression settling model for activated sludge using in-depth batch experiments**. *Water Res* 2008, **42**(3):781-791.

50. Burger R, Diehl S, Nopens I: **A consistent modelling methodology for secondary settling tanks in wastewater treatment**. *Water Res* 2011, **45**(6):2247-2260.

51. Li DH, Ganczarczyk JJ: **Stroboscopic Determination of Settling Velocity, Size and**

Porosity of Activated-Sludge Flocs. *Water Res* 1987, **21**(3):257-262.